Department of the Air Force
Contract AF33(038)-17207

Progress Report on

DYNAMICS OF PARTICULATE MATTER IN FLUID SUSPENSIONS

by

Vito A. Vanoni, En-Yun Hsu, R. W. Davies

Sedimentation Laboratory
Hydrodynamics Laboratories
California Institute of Technology
Pasadena, California

Robert T. Knapp, Director

November 1950 Report No. N-71.1

TABLE OF CONTENTS

I

INTRODUCTION

This report describes work performed during the period from August 1, 1949 to November, 1950. When the project was started, it was financed for one year with the intention of continuing it for a second year, and the program was planned accordingly. However, after about three months of operation, it became necessary for reasons of economy to reconsider the original plans, with the result that the funds for the first year's operation were reduced and plans for continuing the work beyond the first year were dropped. In the early summer of 1950, the U. S. Air Force indicated its interest in sponsoring the work. In view of this prospect, the Office of Naval Research (ONR) allotted funds for an additional three-months' period to allow time for working out the necessary contractual arrangements with the Air Force for continuing the work. These arrangements were worked out and the studies were continued under contract with the Office of Air Research, starting November 1, 1950.

II

THE PROBLEM

The problem of concern in this investigation is an analytical and experimental study of the dynamics of particulate matter suspended in turbulent flows. The practical problems in this field arise in connection with transportation of small particles in the atmosphere and in large bodies of water. In this particular study, attention will be focused on the transportation in liquids, such as water. Analysis and experiments indicate a correspondence between the main aspects of the problem in a liquid and in a gas. Therefore, the results obtained by studies in liquids will also help to clarify the problem in gases.

The transport of particulate matter in a turbulent flow cannot be considered without a knowledge of the state of the motion of the fluid. Of greatest interest is the effect of the turbulence since it is responsible for spreading or diffusing the particles that are carried along in a flow. Therefore, in attacking this problem, considerable time will be devoted to the study of turbulence.

Particles are transported in a flow by the moving fluid itself and by the force of gravity. The fluid motion is composed of a mean motion and a fluctuating motion which in turn is made up of the motions of turbulence and of the molecules. The effect of the molecules can be neglected since they are small compared to the particles, thus leaving only the mean and the turbulent motion of the fluid as the important ones. The effect of the mean motion on transport of particles can be accounted for very simply, and we are left with the turbulent motion as the main problem. The problem is to express the motion of the particles in terms of the turbulent motion. Because of the intimate relationship between turbulent and particle motions, both problems must necessarily be studied together.

III

APPROACH TO THE PROBLEM

In studying this problem, every effort is being made to reduce it to its basic elements and to study these directly. The techniques which are being applied to this study involve injecting materials into the flow and making direct observation of their motion. These materials are liquids which are immiscible in water and break up into droplets when they are introduced into the flow. When the droplets have the same density as the water, they will follow the water motion, thus enabling the turbulence to be studied. When their density is greater than that of the water, they will simulate sediment, such as sand in water or dust in the atmosphere, and when their density is less than that of the water they will simulate a buoyant material, such as air bubbles in water. One of the important objectives of the study is to clarify the mechanism of turbulent diffusion by means of these direct observations and by so doing, to make available information that may assist theoretical workers to clarify further the general problem. This is being done by observing groups of particles visually in low-speed flows and with still and motion pictures in high-speed flows. In order to observe the fluid motion in three dimensions, the motion pictures as well as the still pictures are taken stereoscopically.

The technique outlined above, of using tracers to follow fluid motion and of observing diffusion by following particles in a flow, is peculiarly adapted to liquids and cannot be used in gases because all gases are miscible and a gas does not have a visible surface. The measuring techniques using the hot wire enemometer, which have been so successful in studying the turbulence problem in air, differ from the tracer technique being used in this study. The essential difference lies in the fact that the hot wire

anemometer makes velocity measurements at a point, while the tracer technique allows one to observe trajectories of particles and thus to make a more direct observation of the turbulent motion. There is no intention of duplicating the type of measurement made with the hot wire anemometer since these can best be made with such an instrument. The intention is to exploit those peculiarities of the tracer technique that show promise of yielding some new information that will help clarify the intimately related problems of turbulence and diffusion.

IV

RESEARCH PROGRAM

A. Analytical Studies

The research program of this project covers the combined analytical and experimental attack on the problem. The first step in making the analytical study of the problem was to review pertinent literature on the subject and to attempt to extend existing results to cover the particular problem at hand. In this manner, the analytical results could be used to guide the experimental program. In a later phase of the studies, when more experimental results become available, they will serve to guide the theoretical work. The analytical studies may be divided into two parts. The first of these is the application of generalized diffusion theories to the problem, and the second is the determination of relations between turbulence and diffusion of sediment particles with a view to calculating the diffusion coefficient of the particles.

1. Application of Diffusion Theories

As a first step in applying existing diffusion theories to the problem of diffusion of particles in a turbulent fluid, a fundamental study was made of the mathematical theory of heat conduction. This theory is in many respects similar in structure to what may be the best formulation of the problem of sediment diffusion. Refinements of existing sedimentation theory are thereby suggested and are of several forms. Some of these merit detailed investigation on a theoretical basis.

As a further step, a review was made of the general field of meteorological problems, which are similar and have received much more attention in the past than diffusion of sediment particles. Several improvements[1][2]* of the theory have been found which may be applied more or less directly. Reports of programs of experimental research which have improved understanding of the meteorological processes have been found, which suggest similarly valuable experiments for sedimentation. A summary of the pertinent literature reviewed was incorporated into a project report.[3] In this report, emphasis was placed on the mathematical techniques of diffusion theory which are discussed in terms that can be followed by engineers not versed in advanced mathematics.

A significant fact noted in this body of literature is that questions have been raised in several quarters recently about the correctness of the model, which is usually assumed in formulating a theory of turbulent eddy diffusion. In this connection, it has been pointed out by Priestley and Swinbank[4] that existing theories of turbulent diffusion fail to describe certain commonly observed phenomena such as the almost universal increase of potential temperature[1] with elevation. This led to an examination of the theory, and criticisms were subsequently made on logical grounds. A modified theory[4] has been advanced which seems to explain the previous difficulties. Inasmuch as very similar difficulties are likely to exist in the theory of particle diffusion in liquids, it seems advisable to consider these fundamental ideas briefly at this point.

In older theories it is assumed that an eddy, before it breaks away from its surroundings, is not only at rest relative to them, but also possesses the average values of the diffusing property (temperature, momentum, etc.) appropriate to that level. This disregards the fact that where there are eddies the properties vary from point to point, and even more important, that subsequent motions need not be of a purely random nature; for example, a warm element of air is more likely to start to ascend and to continue to ascend as long as a buoyant force acts on it. Following these ideas, allowance was made for this anisotropy, by the introduction of what has been called the convective component of turbulence. By means of the extension to the theory which results thereby, it appears that a more successful theory has been obtained. Similar deviations from random motion are likely to exist when sand particles are suspended in water,

*Figures in parentheses refer to bibliography at end of report.

[1] The potential temperature, or temperature of an element of air when it is brought adiabatically to a standard pressure, must rapidly approach a constant value, according to the usual theories, and it is characteristic of the atmosphere that this is not observed.

perhaps as a consequence of their relatively greater inertia. Careful analysis will be required to determine what effects are actually present and how they can be handled. It is conjectured, however, that a new mechanism may be found which will be more important than the usual diffusion mechanism in determining the nature of particle diffusion; such a result would be analogous to the finding of Priestley and Swinbank.

On the basis of the review of the meteorological literature, several more general lines of approach to a better theory have suggested themselves. Among these are the following:

(a) It is found in atmospheric diffusion that an improved theory is obtained by abandoning the assumption of constant diffusion coefficients. Further, using coefficients which depend on direction, on space coordinates, and/or by distinguishing between the appropriate diffusion coefficients for solid matter, momentum, heat, and vorticity, may lead to a greatly improved theory of sediment diffusion. An attempt in this direction is facilitated by the existence of experimental data, as well as by general relationships which have been found and successfully applied to atmospheric problems.

(b) Less restrictive assumptions about the process of diffusion are made by considering the effect on the basic equations of the presence of convection and gravity force fields. The more complicated partial differential equations which result have been solved by methods of Laplace Transform (see, for example, Ref. 4), and otherwise applied successfully to atmospheric problems. It seems natural to attempt an application of these theories to sediment transportation problems.

(c) The boundary conditions in turbulent diffusion processes are likely to be significantly more complex than those previously considered and different from those in the fields investigated. Drawing an analogy with the theory of neutron diffusion, Dr. Carl Eckart[2] has suggested an improved form for conditions at boundaries of liquid- and sediment-bed. This idea seems worthy of development into a theory which can be evaluated by making comparisons with controlled experiments.

2. Relation of Turbulence and Diffusion

As a first step in this study, a critical review has been made of modern isotropic turbulence theory. This has led to the formulation of certain basic ideas regarding the problem which do not lead directly to specific solutions, but serve to guide the thinking on the problem. These ideas are presented briefly in this section. A more complete presentation is contained in the appendix to this report.

The facts which are already known about turbulence, particle diffusion, and nonequilibrium statistical mechanics suggest that the various theories which would supposedly explain them have a common background. The conceptual difficulties which are encountered in each are of a similar nature. With this in mind, an attempt has been made to lay the foundations of a general theory of transport phenomena. It has not been anticipated that such a far-reaching ambition will ever be realized, but it does seem likely that a basic philosophy for this project will be attained. No detailed information has been obtained directly by this approach. However, some very definite insight has been obtained as to which special cases are strategic points in this work. It appears likely that any detailed information obtained from these special cases will give an intuitive understanding of the basic theory.

The theory of general Stochastic processes appears to be a common background of these theories from a mathematical point of view. For the time being, however, its practical usefulness is limited to the diffusion problem alone. An adequate theory of turbulence would certainly lead to the further development of Stochastic processes and vice versa.

There are essentially two approaches to defining turbulence and formulating an adequate theory for it. The first is statistical, and in this sense, is related to the theory of Stochastic processes. The second is along lines of hydrodynamical stability. The principal conclusion derived from the statistical approach is that the state of the fluid (equilibrium or degree of nonequilibrium) can be considered only in relation to the statistical characteristics of the instruments used to measure that state. The stability approach indicates that there is no such thing as a most important, or relevant, turbulent solution. Turbulent solutions appear to be representative of an ensemble of statistical properties.

From the review of the existing statistical theories, the conclusion has been reached that while the average of a velocity or energy over a finite time interval is mathematically most inconvenient, it is essential to the physics of the nonequilibrium state. Averages which are mathematically more convenient and rigorous essentially subordinate the nonequilibrium state to final, or equilibrium, states. A heuristic attempt has been made to relate the length of the time interval used in the averages to the de-

[2] In private communication.

gree of nonequilibrium.

With a view to applying our knowledge of turbulence to the specific problem at hand, attention has been concentrated on dilute suspensions of small spherical sediment particles in liquids. The object is to deduce a diffusion coefficient for the sediment in terms of the turbulence properties of the liquid. The procedure is (1) to relate the diffusion coefficient to the random motions of the sediment particles about the average liquid stream velocity, and (2) to determine these random motions in terms of the turbulent velocity of the liquid.

By using methods common in kinetic theory, the following relation between the diffusion coefficient D, the mass and the radius m and a of the sediment particles, the viscosity coefficient μ of the liquid, and the mean square random velocity of the sediment $\overline{v^2}$ has been obtained:

$$D = \frac{m\ \overline{v^2}}{18\pi\ \mu a}$$

The calculation of $\overline{v^2}$, in terms of the turbulence properties of the liquid, is much more complicated. The equations of motion of a sediment particle with respect to the moving liquid must be set up and solved, and then enough must be known about the turbulent motion of the liquid to calculate the mean square velocity of the particle. To date, the equations have been set up in the linear approximation, and solved. This expresses the particle motion in terms of the time Fourier transform of the liquid motion. However, the theoretical and experimental work to date on turbulence yields only the space Fourier transform of the liquid motion. Thus far it has not proved possible to get a connection between these two; the simple connection early postulated by Taylor does not suffice, since it gives the time transform at a point fixed in space, whereas the time transform at a point moving with the average stream velocity is now required.

The principal problem for the immediate future is to calculate this time Fourier transform. It may prove possible to do this by setting up a new statistical theory of turbulence in which the time transform rather than the space transform plays the fundamental role, and this is being attempted.

Once this problem is solved, it will be possible to calculate D in terms of the turbulence parameters, and plan experiments that can be used to explore and possibly confirm existing concepts of turbulence. Beyond this, an important extension would be to the case of non-dilute suspensions of sediment, in which the reaction of the sediment particles back on the liquid motion is significant.

B. Experimental Studies

The experimental studies undertaken by this project during the period covered by this report include preliminary measurements and studies of diffusion in turbulent flows and flume studies of sediment transportation. The diffusion measurements were made with improvised apparatus that was not necessarily suitable for precise measurements. These served to develop techniques and to obtain some preliminary data that is useful in planning the more complete measurements that will be made when the final apparatus becomes available. The flume studies are a continuation of some work that was started at the Laboratory in 1935, and used existing apparatus.

1. Diffusion Measurements

Some preliminary diffusion measurements were made using the tracer droplet technique in an existing water channel with existing photographic equipment. This channel has a glass-enclosed working section 6 in. wide, 12 in. deep and 3 1/2 ft long. This is a low velocity channel with the maximum velocity of about 3 fps.

A number of motion pictures were made of droplets having the same density as water so that they would follow the water motion and thus enable one to observe turbulence. Some of these were taken with a fixed camera and others were taken by rotating the camera at such a rate that groups of droplets were followed down the channel. Since a standard motion picture camera was used, the maximum rate at which pictures were taken was 64 frames per second. These preliminary photographs showed that the turbulent motion could be observed very well, and demonstrated that the technique adopted for the main studies is a very useful one.

The greatest number of observations were taken with a fixed plate camera. These pictures can be divided into three types: first, the single exposure; second, multiple exposures with droplets distributed over the entire field; and third, a large number of exposures on the single plate with only very few droplets in the field.

Fig. 1 is a photograph of the first type. The droplets have been injected at the right and move downstream to the left. The picture shows the position of each droplet at the instant of exposure. The droplets are made of a mixture of

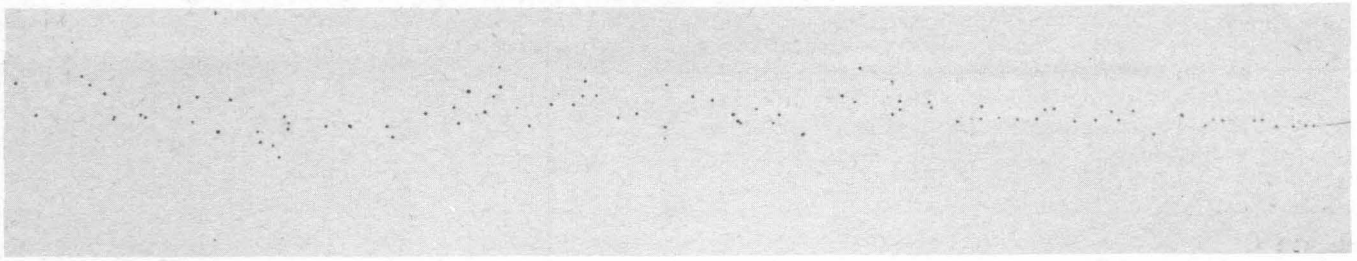

Fig. 1 - Single exposure photograph showing spread of tracer droplets in a turbulent flow. The droplets have been injected into the flow through the small tube at right.

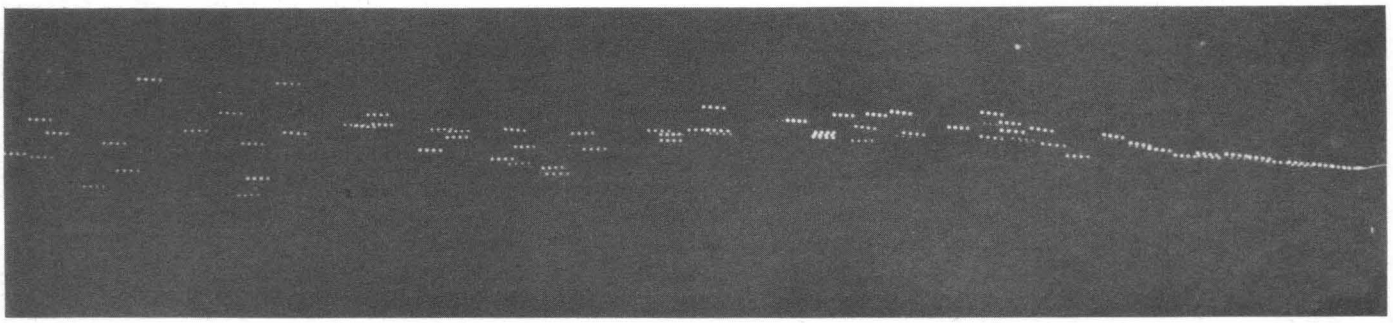

Fig. 2 - A four-exposure photograph of tracer droplets in a turbulent flow. The interval between exposures is 1/100 sec.

caroon tetrachloride and heptane dyed with an oil soluble black dye and are injected into the flow through a small hypodermic needle. The flow, which has an average velocity of about 0.5 fps, has a reasonably high turbulence intensity and also a moderately large scale, as can be seen by the relatively rapid spread of the droplets. The pictures were taken with Edgerton type flash lights which have a flash duration of 1 to 2 microseconds.

The second type of photograph is illustrated in Fig. 2. Four exposures have been taken with an interval of 1/100 sec between each exposure. In this particular picture, the droplets have been made white by mixing the fluid with a small amount of zinc oxide and the photograph was taken against a black background with front lighting. In this manner only the droplets are lighted and very little light from the background is available to expose the film. As can be seen from the picture, the droplets tend to rise, indicating that they are slightly buoyant. Despite their buoyancy, some of the droplets have a downward component of velocity as indicated by the downward inclination of the line joining adjacent images of a droplet.

The third type of photograph is illustrated in Fig. 3(a). A series of over 100 exposures has been taken in this picture, each line of dots representing the path of a droplet across the field of view, which covers the entire length of the working section. As may be seen from the picture, about 10 droplets were in the working section at the time this picture was taken. The graphs in Fig. 3 represent measurements made from the trajectory or path of the lowest droplet in Fig. 3(a) to illustrate the type of measurement that can be made by this method. These were made directly from the negative with a precise measuring engine. The distances x and y appearing on the graphs are those measured directly from the photographic plate. Since the reduction ratio of the photograph is 4.67, the true distance in the channel is obtained by multiplying the distances shown in the graphs by 4.67. No attempt was made to correct for the small effect of the refraction of the glass windows and the water. The scale was obtained from a known distance between two markers which appeared in the photograph. Figure 3(b) is a graph of the trajectory of a droplet with a highly exaggerated vertical scale. Figure 3(c) is a graph of the horizontal velocity u plotted against the horizontal displacement x. The velocity fluctuations show up clearly in this graph. Another fact that is apparent from the graph is that the velocity diminished slightly with distance downstream. This is likely due to the fact that the droplet is moving towards one of the walls where the velocity is being retarded by friction.

Figure 3(d) is a graph of the vertical velocity

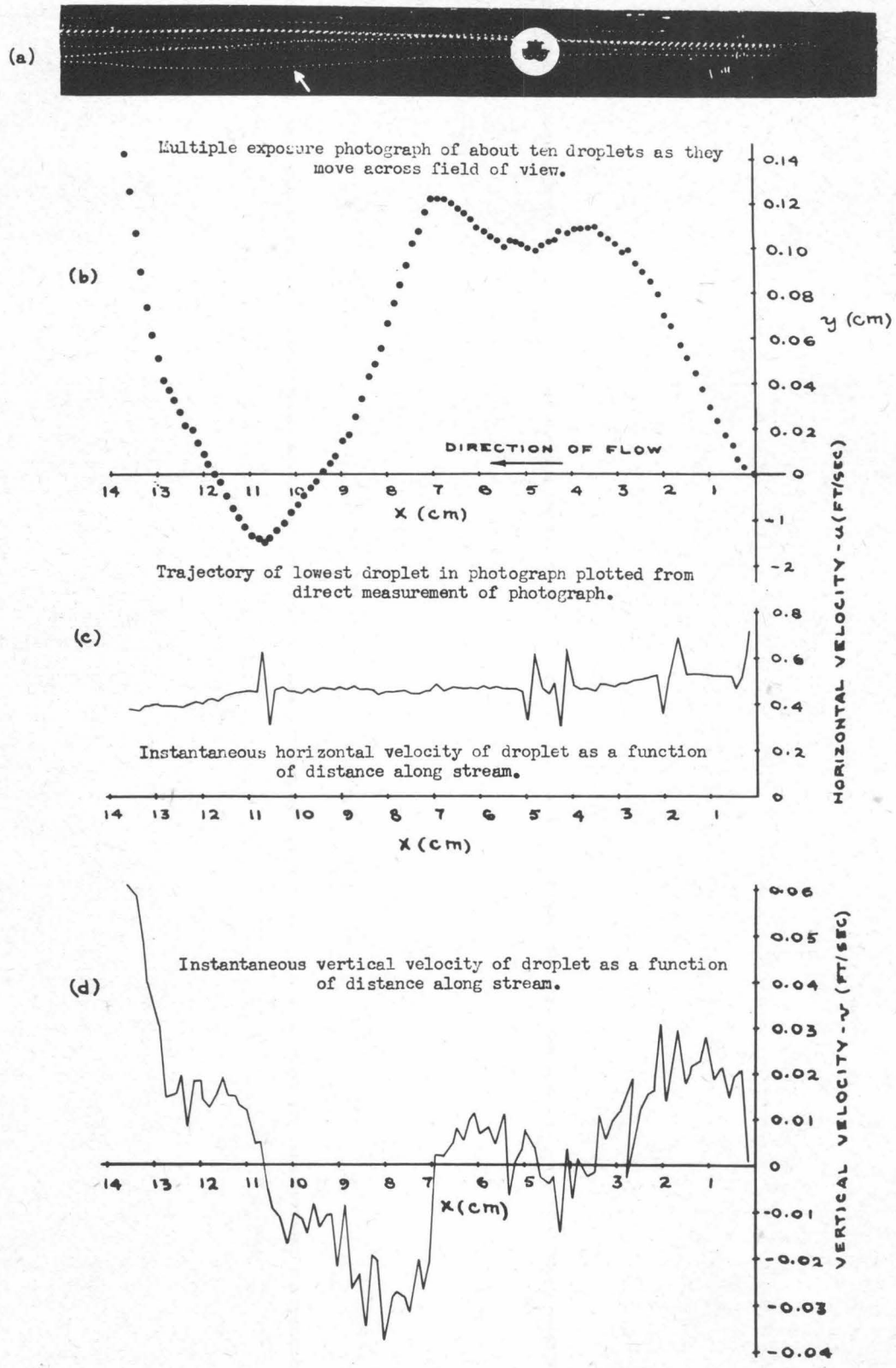

Fig. 3 - Results of observation of turbulent flow using the tracer droplet technique.

component. Since there is no mean flow in this direction, this component gives directly the component of turbulent velocity.

A number of pictures were taken also with color film, using droplets of several different colors at one time. By this means, it is possible to follow droplets from several different sources and to get the relation between the turbulent characteristics at neighboring points.

The pictures in Figs. 1, 2, and 3, which were taken on a single plate, do not permit measurements in the transverse direction normal to the side walls of the channel. Furthermore, measurements made from these pictures are slightly in error because of refraction effects and because the scale varies to some extent with the distance from the camera, and this distance is not known. These difficulties can be eliminated by using stereoscopic pictures. A stereoscopic pair of photographs is shown in Fig. 4. This pair has been mounted so that it can be viewed with the standard table stereoscope used in mapping work. It has been selected not because of any particular value it has in studying the diffusion problem, but because it illustrates some very complicated motions in a flow. A glass tube 1/2 in. in diam. has been placed in the flow with its axis vertical. There is separation of the flow in the wake of the tube which is very complicated and has substantial components of motion normal to the side wall of the channel. These can be seen very clearly when the pictures are viewed with a stereoscope and indicate the practicability of measuring this component of diffusion and turbulent motion by this means. Investigations indicate that the distance from a reference plane, such as the side wall of the channel to a droplet, can be obtained to a high

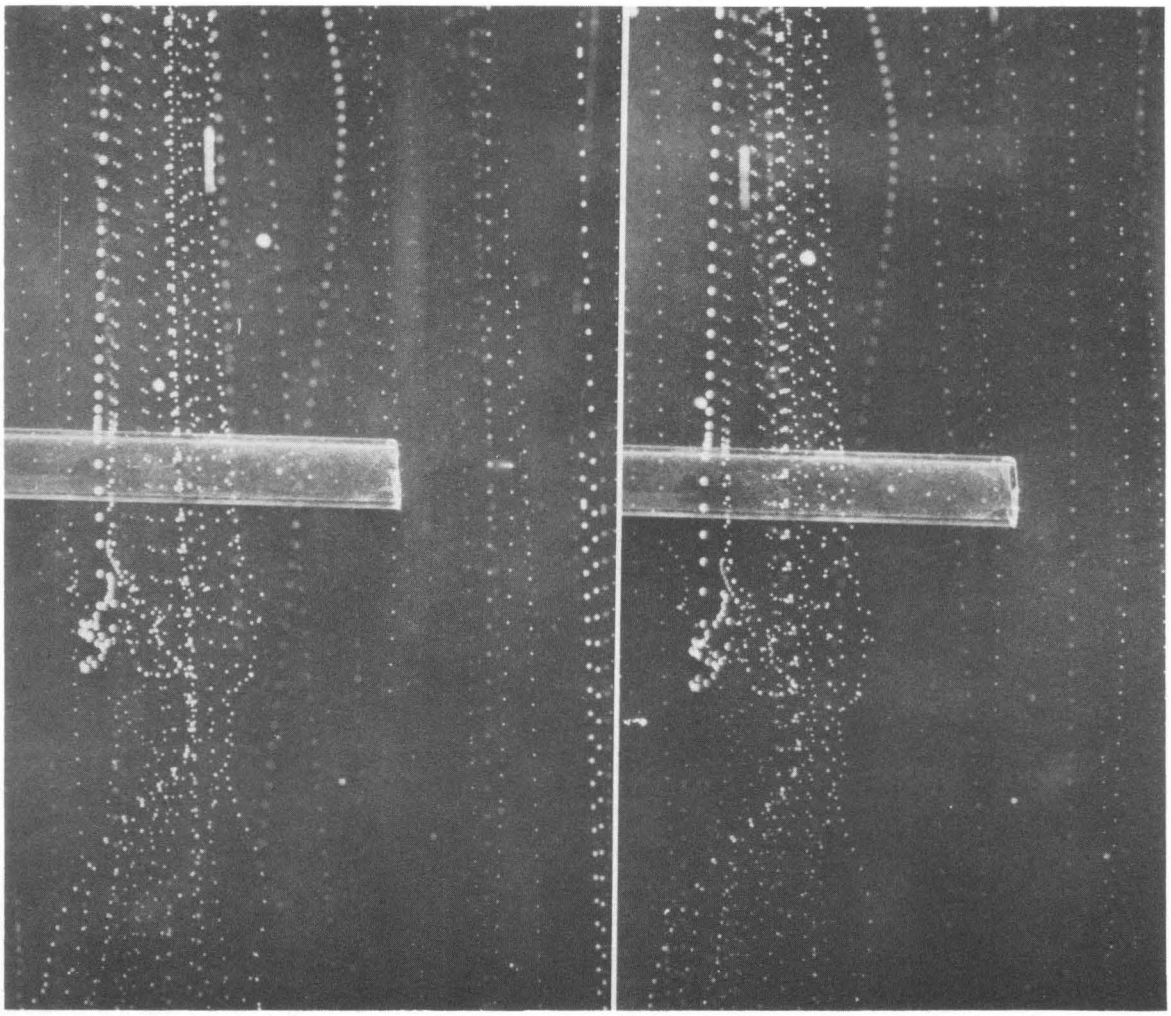

Fig. 4 - Stereoscopic photographs of turbulent flow past a cylinder using the tracer droplet technique to show the flow paths. These pictures may be viewed stereoscopically with a standard stereoscope.

degree of precision by stereoscopic projection. This precision seems to vary very little with the sharpness of the images, and therefore a much greater depth of field can be covered than was first thought possible.

2. Flume Studies of Sediment Transportation

This study is a continuation of a program of sediment studies started in 1935. The flume available for these studies was 33 in. wide and 60 ft long. A photograph of this flume is shown at the right of Fig. 13. The studies are concerned with transportation of material that is suspended in the turbulent flow. The observations are made in the downstream portion of the flume where uniform conditions have been established. The flume is wide enough so that the central part of the flow is not affected by the side walls and two-dimensional conditions therefore exist.

The equation for the distribution of sediment in two-dimensional steady uniform flow is:

$$C\,w + D\,\frac{dc}{dy} = 0 \qquad (1)$$

where C is the concentration of sediment at a distance y up from the bottom, w is the settling velocity of individual grains of sediment in still water and D is the diffusion coefficient for the sediment.

By assuming that D in Eq. (1) is the same as the coefficient for momentum transfer, and that the velocity distribution is given by the Von Karman logarithmic law, the following solution to Eq. (1) is obtained:(5)

$$\frac{C}{C_a} = \left[\frac{d-y}{y} \times \frac{a}{d-a}\right]^z = H^z \qquad (2)$$

where d is the depth of flow, C_a is the concentration at the level y = a, and z is the dimensionless number:

$$z = w/k\sqrt{\tau_o\ /\rho}$$

where k is the von Karman universal constant with a value of approximately 0.4, τ_o is the fluid shear at the solid bottom, and ρ is the density of the fluid.

The early experiments(6) carried out under the sediment transportation program, dealt with fine sands. The experiments planned under the present project were to extend the investigation to coarser sands. A number of experiments with the coarser materials showed that uniform conditions were not established in the flume. Therefore, in order to analyze this condition, it would be necessary to use a more general form of diffusion equation than Eq. (1), which would take into account the change in conditions with distance in the direction of flow. No time was available to work on this particular theoretical problem because of the pressure of the work in the more general diffusion problem. Because of the difficulties encountered and of the limited time available, the flume studies were discontinued.

Figures 5 and 6 show, respectively, velocity and concentration profiles at the centerline of the flume at distances of 30 ft and 45 ft from the inlet to the flume. These observations were made with flow depths of .605 ft, with a channel slope of .0025. In this run (Run 74), the material being transported was the coarse sand which has an average size of 0.25 mm. The mean concentration of the sand in suspension was about 2 grams per liter.

Figure 5, which is a semi-logarithmic velocity profile at the centerline at distances of 30 and 45 ft from the inlet, shows that the velocities at the two stations were the same, and hence that uniform velocity was established between the two stations. It also shows that the profiles fit the logarithmic law which was assumed in deriving Eq. (2). Figure 6, which is a concentration profile, shows that uniform conditions for sediment have not been established.

Figure 7 is a logarithmic graph of the relative concentration C/C_a vs. the function H of Eq. (2) for Run 74, which was made with 0.25 mm. sand, and for Run 38, which was made previously using a sand with a mean size of 0.1 mm. Two facts are readily apparent from the graph. The first is that the measurements with coarse sand plot as curves, while those with the finer sand plot as straight lines. The data that plots as a straight line on this graph follows the theoretical Eq. (2), while the curved lines indicate deviations from this relation. The second fact that is apparent from the curves is that the distribution for the finer material at the two stations is very nearly the same, indicating that uniform conditions have been approached very closely. The measurements for the coarse material, on the other hand, show considerable difference between stations and hence that conditions are far from uniform.

One of the most interesting factors that can be studied in the flume is the effect of the sediment on the flow. To keep the sediment from settling under the force of gravity, work must be done upon it by the cross components of turbulence which suspend it. This means that energy is removed from the turbulence at a faster

rate than in flows that do not carry sediment. Experiments have shown that even with moderate concentrations, the effect of sediment on the flow becomes appreciable. It tends to reduce the so-called apparent, or eddy, viscosity which in turn tends to cause the velocity to increase.

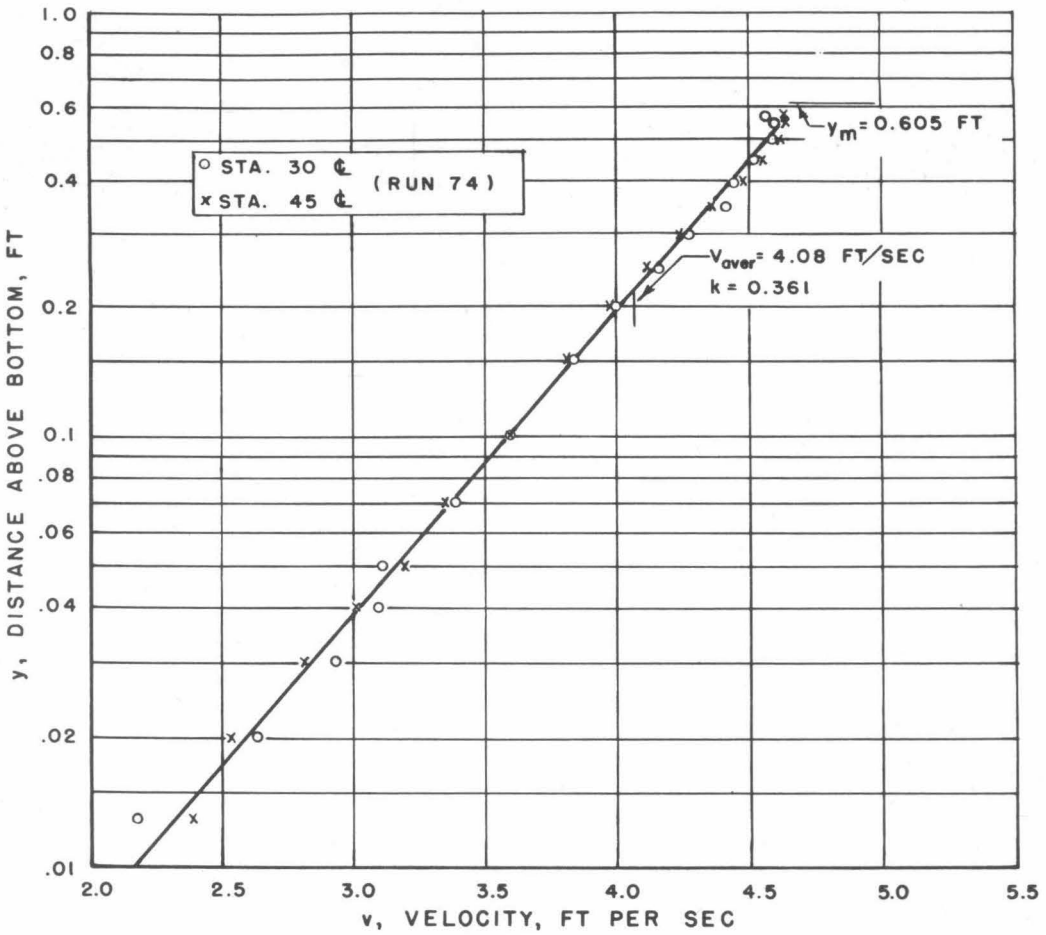

Fig. 5 - Semi-logarithmic graph of velocity profiles on centerline of flume 30 feet and 45 feet from inlet to flume.

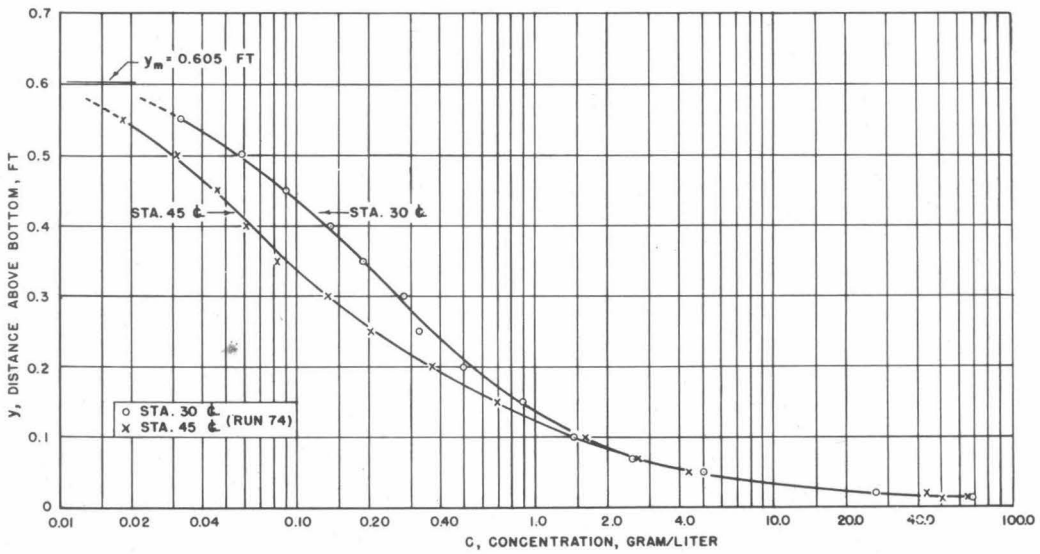

Fig. 6 - Concentration of suspended sand on centerline of flume 30 feet and 45 feet from inlet.

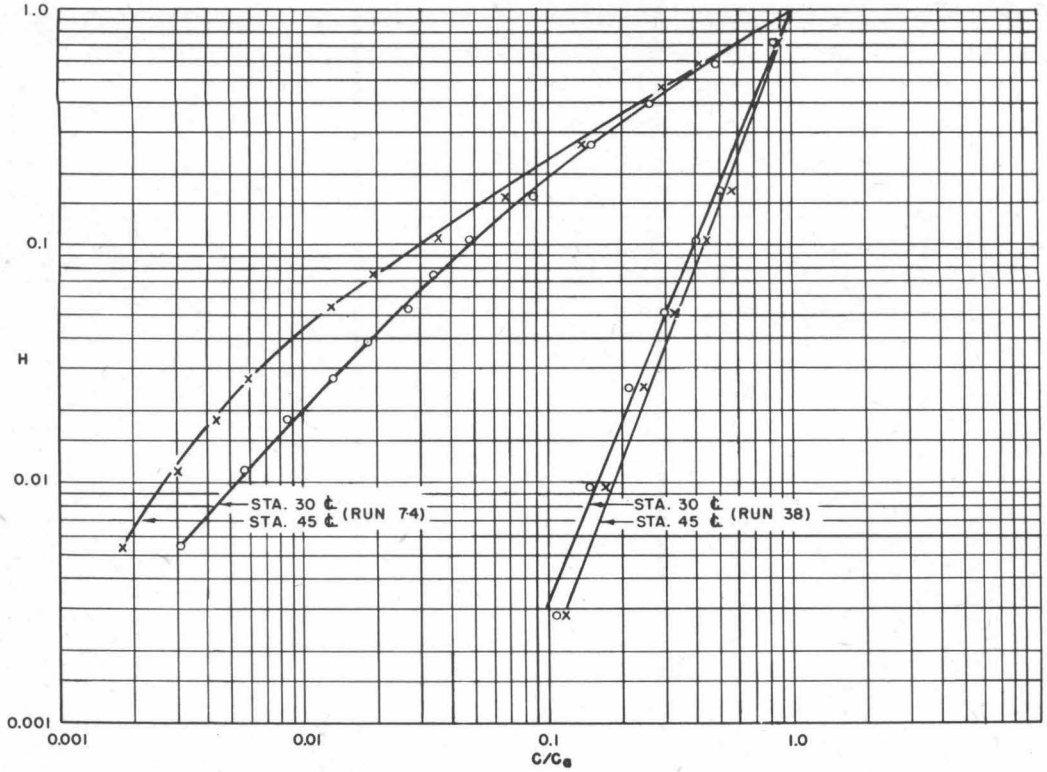

Fig. 7 - Graph of relative sediment concentration C/C_a, versus sediment distribution function, H, for data shown in Fig. 6.

Fortunately, one of the problems of primary interest to this project is the transportation of very small quantities of material in suspension. For such dilute suspensions, the effect of sediment on the fluid motion is negligible and the problem is much simpler than with more concentrated suspensions. As the work of the project progresses, the high concentrations may become of primary interest and it may be desirable to resume the flume studies.

3. Tracer Droplet Techniques

In making preliminary studies of flow with the tracer droplet technique, a number of problems were encountered. Among these were the selection of fluids that would give satisfactory tracers and still not attack the painted and plastic surfaces of the water tunnel, development of means for coloring the droplets, and of methods for controlling the size and spacing of the droplets. This section of the report describes some of these problems and their solution.

Materials for Making Tracer Droplets

Tracer droplets for conducting studies in water can be made of any liquids that are immiscible with water. Since it is necessary to control the density of the droplets, they are usually made of a mixture of two liquids, one of which is lighter and the other heavier than water. Some of the liquid mixtures that were used in the present experiments are shown in Table I.

TABLE I. LIQUID MIXTURES USED FOR TRACER DROPLETS

Light Liquid		Heavy Liquid	
Liquid	Specific Gravity	Liquid	Specific Gravity
Benzene	0.879	Carbon tetrachloride	1.63
Heptane	0.684	Carbon tetrachloride	1.63
Heptane	0.684	Ethylenechloride	1.26

All of the liquids listed in Table I are good solvents and may attack paint that is in the flow system where the droplets are being used. One of the most satisfactory paints for protecting steel against water is a coal tar enamel, also referred to as bitumastic paint. This paint is very soluble in the liquids used for droplets, and could not be used in the water tunnel circuit designed for this study. The inside surfaces of the tunnel were coated with a paint having a vinyl resin base in a ketone and petroleum hydrocarbon solvent. It was found much more resistant than bitumastic paint to the materials

used for tracers, and it is also resistant to ordinary mineral oil which might possibly be used instead of water as a working fluid.

Tests with samples of vinyl resin paint used in the tunnel showed that it was least susceptible to attack by the mixture of heptane and carbon tetrachloride. All of the other mixtures attacked the paint appreciably, and it appeared that they could not be used in the water tunnel circuit.

When single exposure photographs are taken of droplets, back lighting can be used and very satisfactory pictures obtained. Since the liquids making up the droplets have different indexes of refraction than the water, they can be seen easily and photographed. If increased contrast is desired, the bubble can be dyed with ordinary oil soluble dyes.

When multiexposure photographs are desired, front lighting is used and the bubbles are colored with white pigment. A black background is used so that only scattered light from the droplets themselves reaches the camera. The resulting photograph shows the clear white bubbles on a black background, as illustrated in Fig. 3(a). The pigments used to produce white bubbles were white lead, zinc oxide, and titanium dioxide. The white lead tended to settle out very quickly and proved unsatisfactory for this purpose. The other two pigments also tended to settle out to some extent. In order to reduce the settling, emulsifying agents were introduced into the mixture with the pigments. Among the emulsifying agents tried were: potassium ethyl xanthate, triethnolamine, oelic acid, and detergent soap. The last of these emulsifying agents was the most successful. In these experiments, the detergent household soap powder sold under the trade name "Tide" was used. Best results were obtained when the detergent powder was dissolved in n-amyl alcohol before adding it to the mixture of the droplet liquids and pigment. When the mixture of carbon tetrachloride and heptane was treated in this manner, it was found that both zinc oxide and titanium dioxide pigments remained in suspension in sufficient concentrations to color the drops for about four hours. However, the titanium dioxide precipitate tended to form a cake which was very hard to shake loose. On the other hand, the zinc oxide which settled could easily be put back into suspension by shaking gently. For this reason, the zinc oxide pigment was considered more satisfactory than the titanium dioxide. The ointment form of zinc oxide, sold commercially for medicinal use, was found to give good results. To prepare the mixture, about four grams of zinc oxide ointment were added to each 100 cc. of heptane and mixed by stirring. Carbon tetrachloride was then added until the desired specific gravity was reached. This mixture was then shaken until well mixed and 2 cc. of detergent powder dissolved in n-amyl alcohol was added for each 100 cc. of mixture.

No difficulty was experienced in suspending the zinc oxide pigment in a mixture of ethylene chloride and heptane. The pigment was mixed in by shaking without the use of an emulsifying agent and allowed to stand about 12 hours. Some of the coarser particles settled out during this time, but the rest of the pigment seemed to remain in suspension almost indefinitely. In cases where there is no problem of protecting paint, the mixture of heptane and ethylenechloride would be very satisfactory as a tracer fluid.

Before a final selection was made of liquids for tracers, an investigation was made of the effect of liquids on the plastic windows of the working section. The working section is designed to be transparent on all four sides. The top and bottom windows are to be made of the plastic, methyl methacralate, which is sold in the United States under the trade names of "lucite" and "plexiglas". The side windows are to be made of plate glass and, therefore, are in no danger of being attacked by the tracer fluids.

Tests were made by immersing a 1/4-in. diameter rod of lucite in each of the liquids that were considered suitable for use in preparing the mixture for the tracer fluid. The diameter of each rod was measured with a micrometer before immersion and after being immersed in the liquid for 48 hours. The results of these tests are shown in Table II. This table shows that ethylenechloride is by far the most active substance. It also shows that the benzene and and bromobenzene attacked the lucite very actively and, therefore, are not suitable for use where they may come in contact with this material. The heptane and carbon tetrachloride did not attack the lucite and are, therefore, acceptable as tracer fluids as far as this particular feature is concerned.

Injection of Tracer Droplets into Flow

In order to make the most effective use of the droplet technique, it is necessary to control the size and the spacing of the droplets. This problem was investigated analytically and experimentally in connection with developing techniques for injecting the droplets.

Figure 8(a) is a schematic diagram of an injection apparatus of the gravity type, which was used in developing injection techniques. The tracer fluid is injected into the flow through a

small tube pointing in the direction of the flow. The rate at which the fluid is injected can be controlled by adjusting the difference in elevation h between the free surface of the flow and the surface of the tracer fluid in the reservoir. Other variables in this system are the size and shape of the injection tube and the flow velocity in the channel.

The size of the droplet leaving the injection tube can be determined analytically. When the droplet leaves the injection tube (Fig. 8(b)), the drag force on the droplet due to the flow must equal the surface tension force which tends to

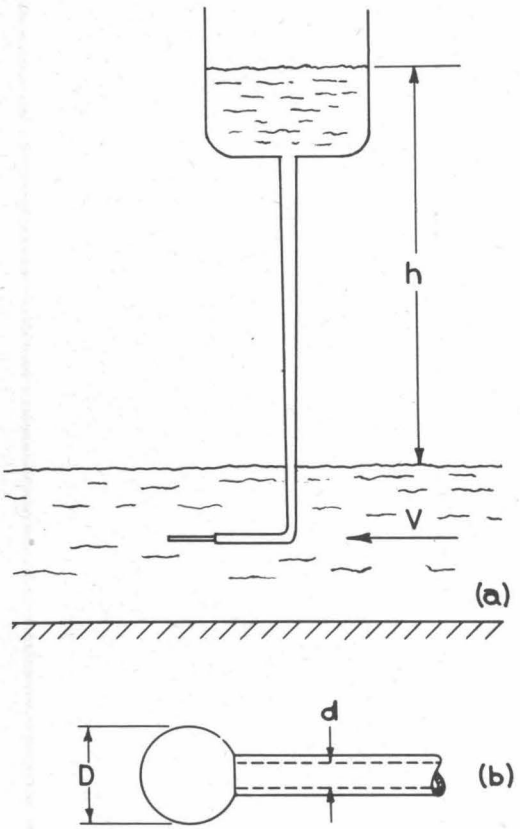

Fig. 8 - Schematic diagram of droplet injection apparatus.

hold the droplet to the tube. This may be expressed algebraically as

$$C_D \frac{1}{2} \rho V^2 \frac{\pi D^2}{4} = \pi d T \qquad (3)$$

where C_D, ρ, V, D, d, and T are, respectively, the drag coefficient of the bubble, the mass density of the water, the flow velocity of the water, the diameter of the bubble, the inside diameter of the injection tube and the surface tension between the tracer liquid and the tube. Equation 3 may be rewritten as:

TABLE II. RESULTS OF TESTS TO DETERMINE THE EFFECT OF TRACER FLUIDS ON LUCITE

Liquid	Diameter of Lucite Rods		Reduction (diam. - inches)
	Before Immersion (inches)	After 48-hr. Immersion (inches)	
Normal Hexane	0.250	0.250	0.000
Heptane	0.250	0.250	0.000
Tolvene	0.249	0.209	0.040
Xylene	0.247	0.244	0.003
Benzene	0.247	0.180	0.067
Dibutyl-phthalate	0.250	0.250	0.000
Bromo-benzene	0.252	0.170	0.082
Carbon tetrachloride	0.252	0.252	0.000
Ethylene-chloride	0.250	0.000	0.250

$$\frac{D}{d} = \sqrt{\frac{8}{C_D W}} \qquad (4)$$

where $W = \frac{V^2 d}{T/\rho}$,

and is known as the Weber number of the system. Since the surface tension is a constant, the following form of the equation may be more convenient:

$$DV = \sqrt{\frac{8dT}{C_D \rho}} \qquad (5)$$

The drag coefficient, C_D, may be estimated by assuming the droplet to be spherical and, therefore, will be approximately a constant for small ranges of flow velocity. Therefore, the graph of the diameter of droplet vs. the stream velocity is approximately a hyperbola. For a given injection system the diameter of the droplet is determined by the stream velocity V, since the quantities T, C_D, and ρ are constant.

The spacing between successive droplets can also be estimated analytically. Let t be the time interval between the departure of the droplets from the injector and v be the velocity of the tracer fluid in the injection tube. Then:

$$vt \frac{\pi d^2}{4} = \frac{\pi D^3}{6} \qquad (6)$$

or $$t = \frac{2}{3}\frac{D^3}{vd^2}$$

Let s be the spacing of the droplets near the injector. Then:

$$s = Vt = \frac{2}{3}\left(\frac{V}{v}\right) d \left(\frac{D}{d}\right)^3 \qquad (7)$$

It may be seen from the above equations that the spacing between droplets is inversely proportional to the velocity v in the injection tube which, in turn, will be directly proportional to the head h (Fig. 8(a)) on the injector system since the flow is laminar.

Experiments were made in which the size and spacing of the droplets of a mixture of carbon tetrachloride and heptane were observed as a function of head h and velocity V for two different injection tubes. One of the injection tubes was made of hypodermic tubing with an inside diameter d of 0.007 in. and an outside diameter of 0.016 in. The end of the tube was tapered very slightly over a distance of about 1/4 in. The second injection tube had an inside diameter d of 0.005 in. and an outside diameter of 0.16 in., and was cut off squarely at the tip. The observations were made in a glass-walled channel 6 in. wide and 12 in. deep. Figure 9 is a typical photograph from which the measurements of bubble size and spacing were made. The spacing was measured near the injection point before the scattering effect of the turbulence had time to act on the droplets. The measurements were made directly on the negative with a precision tool maker's microscope. The scale of the photograph was determined directly by photographing a machinist's rule in the channel. The droplets were dyed black with an oil soluble dye.

The experimental results are shown in Figs. 10 and 11 for the 0.007-in. and 0.005-in. diam. injection tubes respectively. Figures 10(a) and 11(a) show the relationship between the diam. D of the droplet and the stream velocity V. The experimental relationships closely approximate hyperbolas and in this respect agree with Eq. 3. It is interesting to note that the diameter of the droplet approaches a constant value of 0.023 in. and 0.025 in., respectively, for the 0.007-in. and 0.005-in. injection tubes for stream velocities greater than 2.5 fps. The 0.007-in. needle is tapered at the end, and therefore has less contact circumference than the 0.005-in. needle. This probably accounts for the fact that the tube with the larger inside diameter produces the smaller bubbles.

Figures 10(b) and 11(b) show the relationship between the spacing of the droplets and stream velocities for different values of h, the head on the injection system. As may be seen from the graph, for a given injection tube and stream velocity, the smaller the value of h, the larger will be the droplet spacing. This relationship is evident from Eq. 7, which states that for a given value of the flow velocity V, the spacing is inversely proportional to v and hence to h.

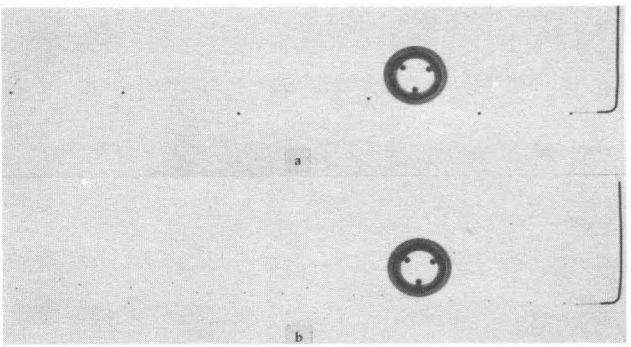

Fig. 9 - Photographs showing droplets injected into flow. The inside diameter of the injector tube is 0.005 in. and the head h on the injector system is 1.50 ft.
(a) Channel velocity is 0.44 fps.
(b) Channel velocity is 1.13 fps.

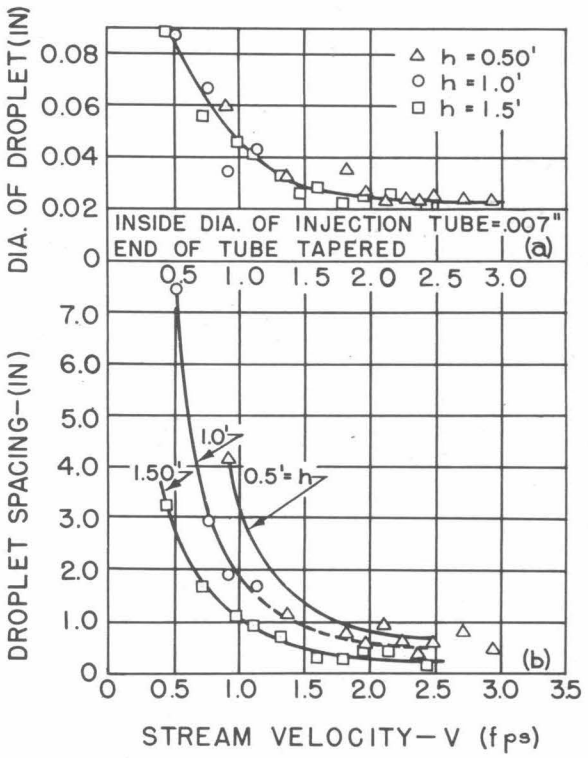

Fig. 10 - Relation between stream velocity, size and spacing of droplets, and rate of injection of tracer fluid for an injection tube 0.007 in. in diameter.

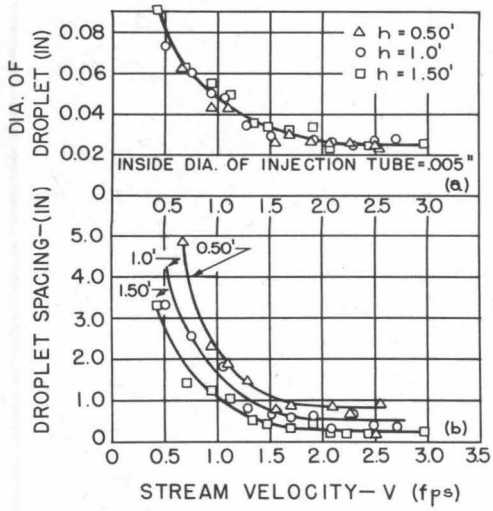

Fig. 11 - Relation between stream velocity, size and spacing of droplets, and rate of injection of tracer fluid for an injection tube 0.005 in. in diameter.

V

DEVELOPMENT OF APPARATUS

A. Low Turbulence Water Tunnel

The main apparatus planned for carrying on studies of transportation and diffusion is a water tunnel which has been designed to give a low turbulence level in the working section. With this tunnel, the intensity and scale of turbulence can be controlled and the effect of these factors on the transport and diffusion of particles studied. It is also possible to study the effect of turbulence in boundary layers formed at the walls of the working section or on a plate inserted in the working section.

Figure 12 is a diagram of the tunnel which has a working section 12 in. square by about 8 ft long. The working section will have glass and transparent plastic windows on all four sides to permit visual and photographic observations. The maximum flow velocity in the tunnel is about 15 fps. To obtain low turbulence in the working section, the design practice developed in research with wind and water tunnels was followed. Turning vanes were used at all corners and small divergence angles were used in expanding sections where the flow is decelerating. A high efficiency pump was used and provision was made for turbulence damping screens and a settling chamber just upstream from the nozzle. The nozzle contracts from 4 ft square to 1 ft square thus giving an area contraction ratio of 1:16. As shown in Fig. 12, provision has been made for introducing turbulence grids at the inlet to the working section. By varying these grids, the scale and intensity of turbulence in the working section also can be varied. The working section increases slightly in cross section in the direction of flow to allow for growth of the boundary layer at the walls without increasing the average velocity in the core of the flow. The over-all length of the tunnel is slightly over 40 ft. All of the parts of the circuit, except the working section, nozzle and the short section of the diffuser following the working section, are made of mild steel plate. The working section consists of a steel framework which holds lucite and glass windows. The nozzle and short diffuser are made of cast brass and are machined inside. The tunnel circuit is designed for a maximum pressure of 15 psi gage. The interior surfaces of the steel portion of the tunnel circuit were sandblasted and painted with 5 coats of paint having a vinyl resin base.

The circulating pump for the tunnel is of the standard mixed flow type and is driven by a direct current electric motor through a V-belt transmission. Power for the motor is furnished by an electronic rectifier. The speed of the motor can be set to get the desired velocity in the working section by means of an automatic speed control device which maintains the speed, and hence the flow velocity, very accurately.

The tunnel is located in the Sedimentation Laboratory at a site made available by removing an existing flume. Figure 13 is a photograph of the Sedimentation Laboratory taken before work was started on this project. The site of the water tunnel is at the left background of the picture. The flume shown at the left in this picture was removed to make room for the tunnel. The flume shown at the right is the one that was used for the flume studies of sediment transportation referred to earlier in this report.

Figure 14 is a photograph taken in November 1950 when the tunnel was only partially erected. This view is taken looking in the upstream direction; the nozzle and the working section have not yet been erected. At the right of the photograph is shown the diffuser section which is immediately downstream from the working section. This portion, which is unpainted in the picture, is made of stainless steel and is in four sections bolted together so that the entire inside surface could be machined before assembly. This diffuser expands from a section of 14 3/4 in. square to 24 in. square with an included angle between opposite sides of 3° 13'. Figure 15 is a photograph of the tunnel during an initial stage of erection. In the foreground is the 4-ft square elbow in the lower reach of the tunnel circuit. The vanes in this elbow can be seen clearly. These are made of 1/4-in. steel plate and are spaced about 3 1/2 in. apart horizontally and have a chord distance from leading edge to trail-

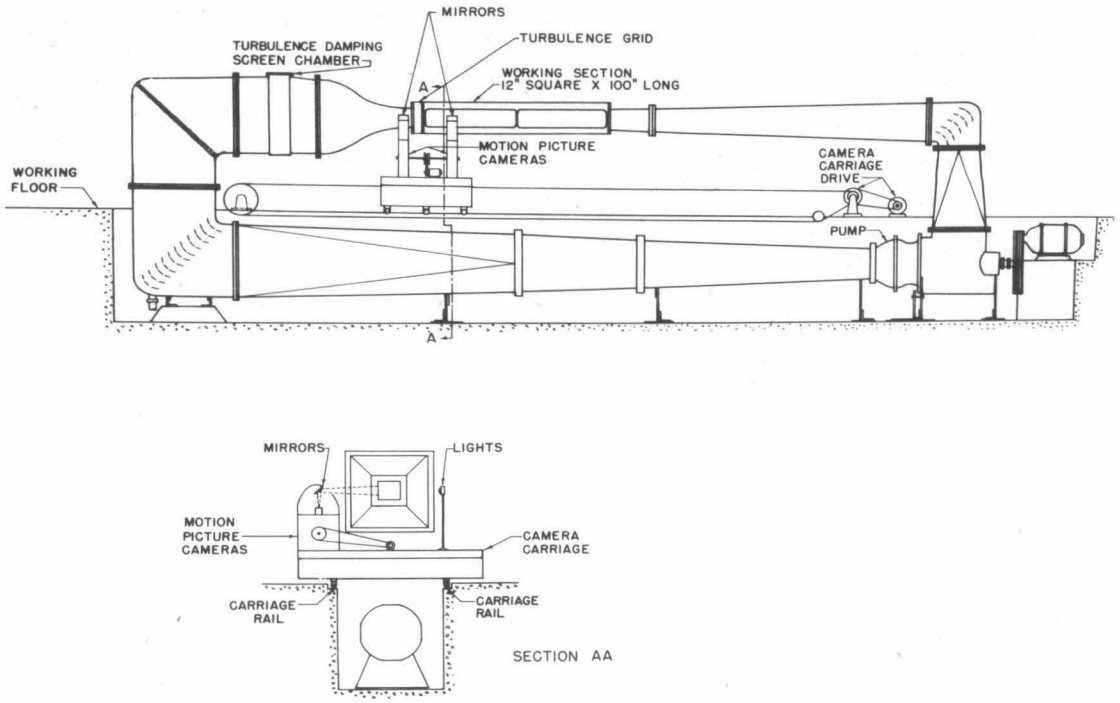

Fig. 12 - Diagram of low turbulence water tunnel.

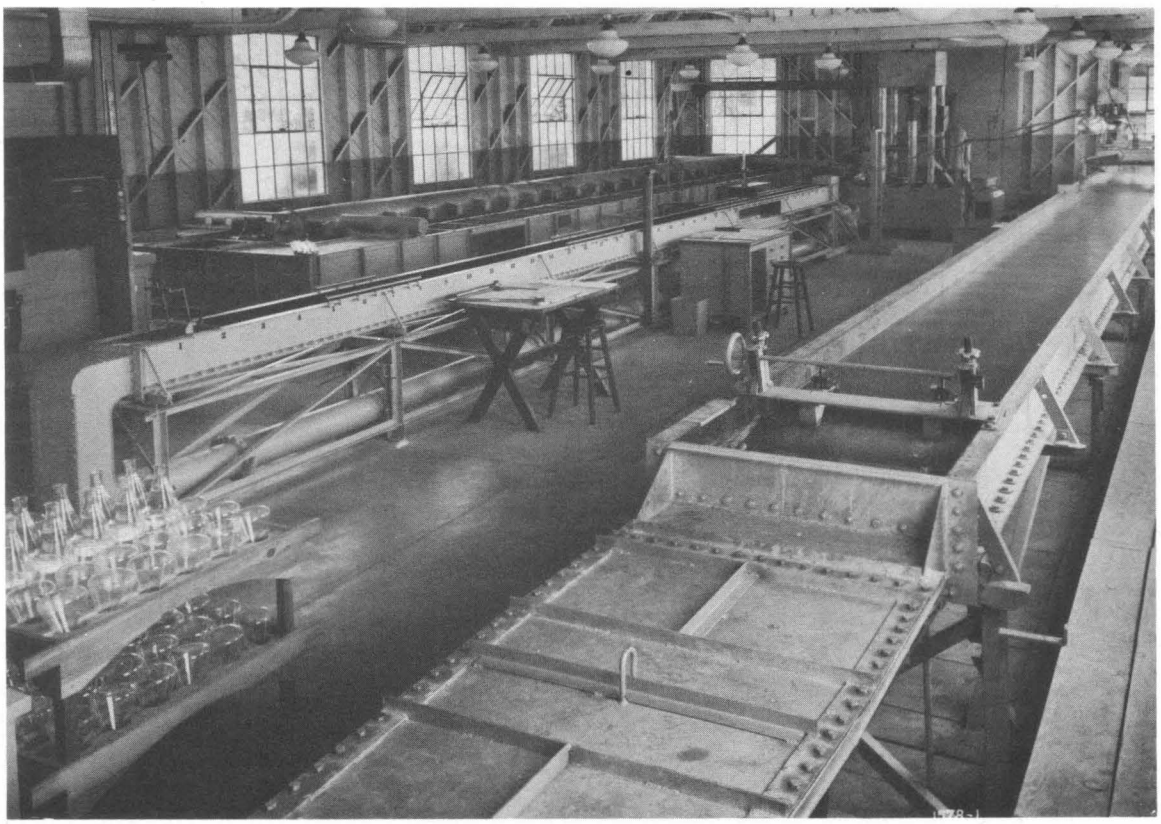

Fig. 13 - Photograph of Laboratory before water tunnel was installed.

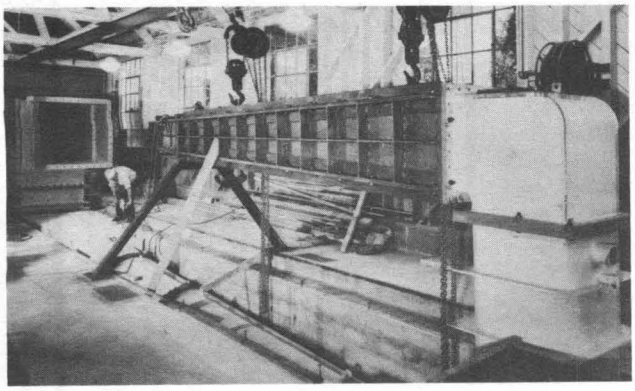

Fig. 14 - View of tunnel when erection was only partially completed.

ing edge of about 11 in. Immediately back of this elbow is shown the expanding section which bolts to the vertical face of the elbow shown in the foreground. This particular piece forms the transition from the circular section to the square section. In the right background of the picture is shown the upper elbow of the circuit which bolts to the horizontal flange of the elbow shown in the foreground. Attention is called to the reinforcing ribs on the exterior of the elbow which are necessary to resist the interior pressure of the water. Figure 16 is another photograph of the upper elbow of the circuit which precedes the nozzle (see Fig. 12) and which also was shown in Fig. 15. Attention is called to the close spacing of the vanes which are seen clearly in this photograph. These are made of 1/4-in. steel plate and are spaced approximately 1 in. apart measured parallel to the plane of the flanges of the elbow and have a chord distance measured from leading edge to trailing edge of 2 7/8 in. The leading edges of the vanes were rounded off approximately to a circular cross section and the trailing edges have been tapered down to a thickness of about 1/8 in. The vanes in this elbow are spaced much closer than in the one immediately upstream. To eliminate as much as possible any large scale disturbances, provision has been made for a honeycomb immediately downstream from this elbow. As shown in Fig. 12, a chamber is provided downstream from the elbow for inserting screens for damping out turbulence before flow goes into the nozzle.

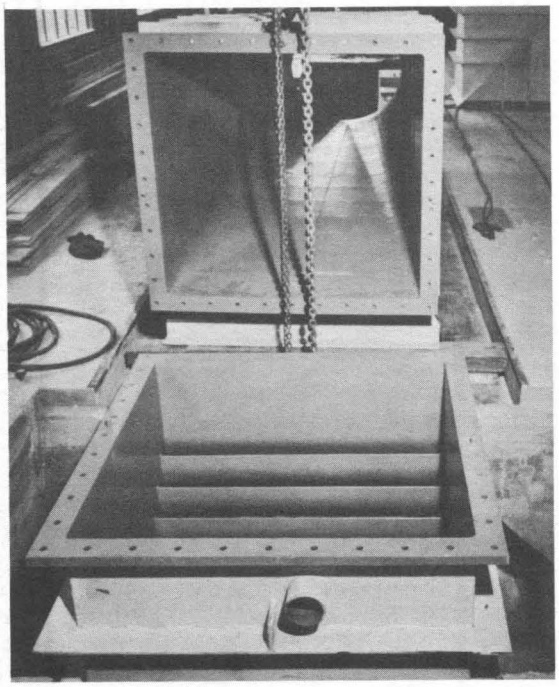

Fig. 15 - Water tunnel in an initial stage of erection showing transition diffuser from circular to square cross section in background and lower vane elbow in foreground.

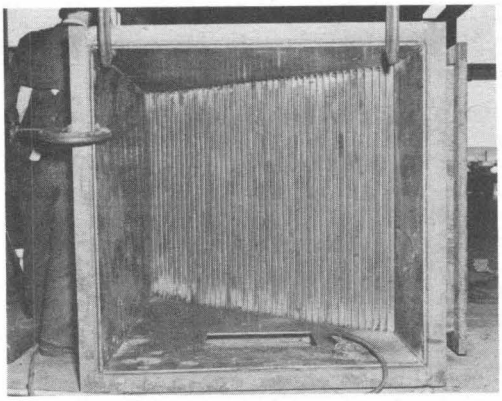

Fig. 16 - View of upper elbow which precedes nozzle, showing closely spaced vanes for turning flow.

Figure 17 shows the elbow just upstream from the pump. This elbow which is 32-in. diam. carries the outer bearing for the pump shaft. The housing for this bearing is shown at the left. Figure 18 is a photograph of the steel framework for the working section. In this view, the downstream end of the working section is towards the camera and the entire section has been rotated 90° so that the horizontal openings in the picture will be vertical when the working section is installed. It will be noted that the far end of the working section is square and that the near end is rectangular. The finished inside dimensions of the working section will be 12 in. by 12 in. at the upstream end and 12 in. by 14 in. at the downstream end. The section is increased in the downstream direction so that the boundary layer may develop without increasing the velocity in the core of the flow.

The total friction loss in the water tunnel circuit without turbulence grids for the maximum design velocity in the working section of

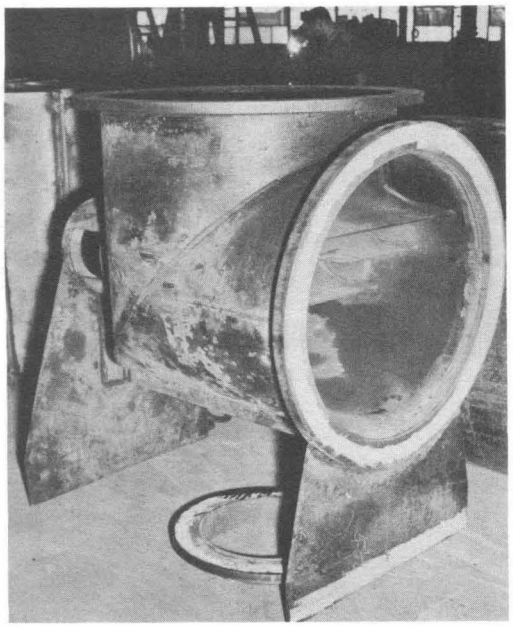

Fig. 17 - Pump elbow.

15 fps was calculated to be 1.32 ft of water. The energy ratio calculated from these quantities is 2.65 where the energy ratio is defined as the ratio of the power represented in the kinetic energy of the flow in the working section to the power input to the water necessary to circulate the flow. This is also equivalent to the ratio of the velocity head in the working section to the head loss in the tunnel circuit.

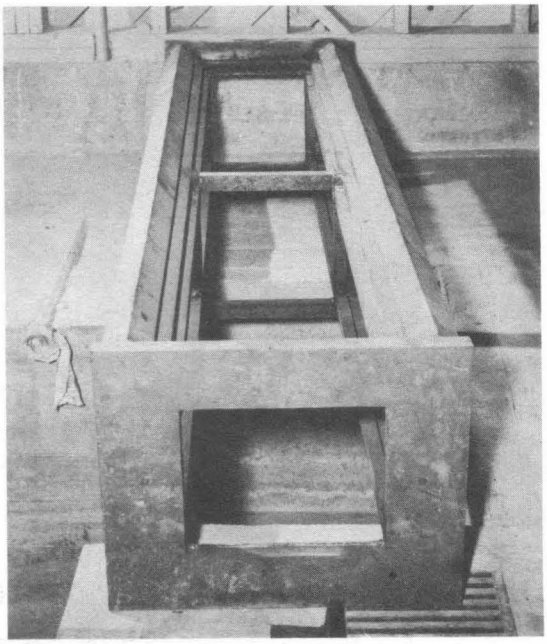

Fig. 18 - Unmachined framework for working section.

Figure 19 is a graph showing the pump characteristics for a constant rate of flow of 15 cfs which is the flow rate for a working section velocity of 15 fps. The graph shows that to obtain a head of 1.32 ft, the speed of the pump will have to be about 217 rpm and the efficiency will be about 71 per cent. Most of the runs will be made with turbulence grids at the inlet to the working section, which will increase the resistance and hence the total head developed by the pump. It is estimated that the resistance of the turbulence grids will be from 1 to 2 velocity heads, which will increase the total head developed by the pump to between 4.8 and 8.3 ft. It is seen from the graph that if the head is 4.8 ft, the efficiency will be 88 per cent and if the head is 8.3 ft, the efficiency will be 83 per cent. All of these efficiencies are high and thus indicate that this machine is well adapted to the water tunnel application.

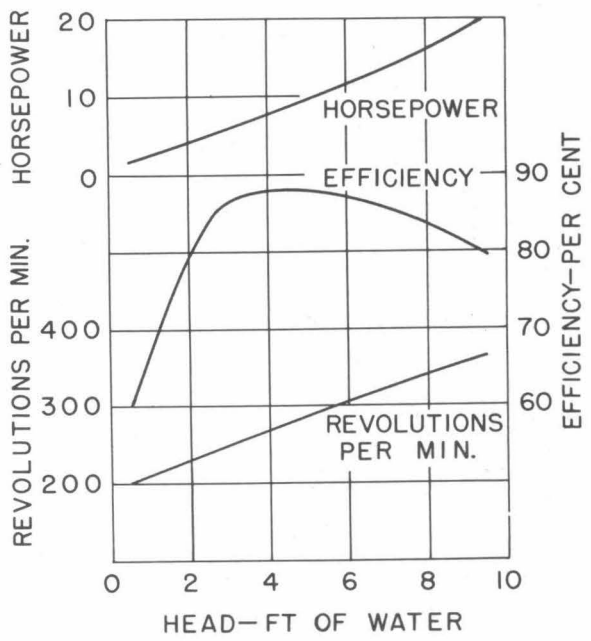

Fig. 19 - Characteristics of water tunnel pump for a constant discharge of 15 cfs.

The power for the direct current electric motor which drives the water tunnel pump is furnished by a rectifier unit. This unit has an input of 220-volt, 3-phase alternating current and an output of direct current varying between 0 and 50 volts. Variation of the output is accomplished by three continuously variable auto transformers (Amertran transtats). Figure 20 is a photograph of the partially completed rectifier unit. The three auto transformers are shown on the two lower shelves and the rectifying tubes are shown on the upper shelf.

B. Optical and Photographic Apparatus

Stereoscopic pictures with fixed plate cameras will be taken as described earlier in this report. A camera which has been designed for making this kind of photograph is shown in Fig. 21. It is made of two cameras mounted on a common base. The distance between the cameras is about 30 in. The lenses are pointing toward the axis of symmetry of the pair so that the angle of intersection of the lens axes is 45°. This large angle of intersection was used so that high accuracy would be obtained in locating the droplets in the third dimension. The stereoscopic camera will cover a field 12 in. high by 36 in. long. Glass photographic plates are used because they remain flat and do not distort. The data desired from the photographic negatives are the locations of the droplets in the working section as a function of time. To obtain these data, analyzers will be built which re-project the stereoscopic pictures back through a system that is identical with the taking system. For instance, identical lenses will be used in the projectors and in the cameras, and the optical path of the light will be duplicated by having water and glass in the analyzer system just as in the taking system. To determine the position of a droplet in such an analyzer, a target is moved in space until the images from the two projectors are sharply focused at a single point on the target. The coordinates of the droplet are then read from scales attached to the carriage holding the target.

Lights for both the motion- and fixed-plate photographs are of the Edgerton flash type which have been used extensively in the Hydrodynamics Laboratory[3] for a number of years. The flash duration for these lights is from 1 to 2 microseconds. The rate of flashing can be controlled accurately so that the time interval between exposures is known very precisely. The quotient of the distance moved by the tracer during the interval and the time interval gives the instantaneous velocity.

Fig. 20 - Partially completed rectifier unit for producing direct current for pump motor.

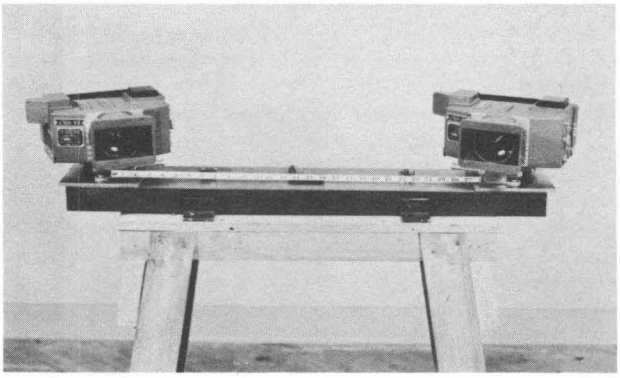

Fig. 21 - Stereoscopic camera.

C. Status of Design and Construction

As of October 31, 1950, the main parts of the tunnel were as shown in Fig. 14. In addition, the nozzle was about 90 per cent completed. The metal framework for the working section had been built (Fig. 18) but was not yet machined. The motor, transmission, and the rectifying unit, which supplies direct current for the motor, were available for installation.

A fixed plate stereoscopic camera (Fig. 21) was built and a number of preliminary pictures were taken with it. Designs for the motion picture cameras and for the carriage and drive for the motion picture cameras were almost completed and some of the material for this part of the apparatus had been purchased. Some preliminary sketches had been made for the analyzer for the motion pictures and fixed plate pictures.

[3] For a more complete description of the flashlights and stroboscopic photography techniques see Ref. 8.

BIBLIOGRAPHY

1. Sutton, O. G., Quarterly Journal Meteorological Society, London, Vol. 75, 1949. p. 335.

2. Calder, K. L., Quarterly Journal of Mechanics and Applied Mathematics, Oxford, Vol. II, 1949, p. 153.

3. Michelson, Irving, "Theoretical Considerations on Turbulent Diffusion and Sedimentation," California Institute of Technology, Hydrodynamics Laboratory Report N-71, October, 1950.

4. Priestley, C. H. B. and Swinbank, W. C., Proc. of the Royal Society, A, London, Vol. 189, 1947, p. 543.

5. Jaeger, J. C., Quarterly of Applied Mathematics, Vol. III, 1945, p. 210.

6. Rouse, H., "Fluid Mechanics for Hydraulic Engineers," McGraw-Hill, 1938.

7. Vanoni, Vito A., "Transportation of Suspended Sediment by Water," Trans. Amer. Soc. Civil Engineers, Vol. III, 1946, p. 67.

8. Knapp, R. T., Levy, J., O'Neill, J. P., Brown, F. B., "The Hydrodynamics Laboratory of the California Institute of Technology." Trans. Amer. Soc. Mechanical Engineers, Vol. 70, No. 5, July 1948, pp. 437-457.

- APPENDIX -

THEORETICAL CONSIDERATION OF:-

A. SEDIMENT DIFFUSION IN TURBULENT FLOWS

B. TURBULENCE IN A RECTANGULAR BOX

by

R. W. Davies

A. SEDIMENT DIFFUSION IN TURBULENT FLOWS

It is the object of this section to discuss what happens to a large number of small grains suspended in a very irregularly moving fluid. The problem is not easily formulated, so we will begin by pretending that we are able to observe a domain filled with fluid and grains. It is obvious, of course, that motion of the grains is intimately connected with the fluid motion, but the nature of this intimacy is not altogether clear and, what is more important, the motion of the fluid is probably more complex than that of the grains. So it is natural to ask ourselves what we can say about the grains without immediately referring to the motion of the fluid.

In theory we have three experimental techniques at our disposal. The first would be to watch the motion of one or a few grains for a very long time, i.e., long enough to be commensurate with its entire life history. This is the biographical method. The second approach is to observe what occurs in a specific small domain for an infinite length of time. This is the geographical method. Thirdly, there is the possibility (in theory) to observe what happens at a particular point at a specified time an infinite number of times by repeating the experiment. This is the ensemble or trial method.

Now it is frequently assumed that the observational results we get by any of these methods or combinations of them are consistent with each other. This is a very strong assumption if viewed through the mathematician's eyes, but that does not make it any less necessary to the physicist.

Let us momentarily confine our attention to a locale V described as

$$V = \int_{x_0}^{x_1}\int_{y_0}^{y_1}\int_{z_0}^{z_1} dx\,dy\,dz \qquad \text{or} \quad (1)$$

$$V = \int_{\mathcal{X}_0}^{\mathcal{X}_1}\int\int\int d\mathcal{X} \qquad (2)$$

Suppose at some time t_1, we find within V exactly n grains. Now n is in some way related to the volume V. We conveniently define a function $\rho(xyz;t_1)$ such that

$$n(t_1) = \int_{x_0}^{x_1}\int_{y_0}^{y_1}\int_{z_0}^{z_1} \rho(xyz;t)\,dx\,dy\,dz \qquad (3)$$

for all $x_0y_0z_0$ and $x_1y_1z_1$, $\rho(\mathcal{X},t) \equiv \rho(x,y,z;t)$ can be interpreted either as a number density of grains or as a probability distribution. If N is the total number of grains in the fluid universe at our disposal, then $\frac{\rho(xyz;t)}{N}$ is the probability that a grain is in the volume increment $(xyz\,;x+dx,y+dy,z+dz)$. It has been implied in the foregoing that the total number of grains is large, and that if we could determine $\rho(x,y,z;t)$ for almost all (x,y,z), we would be in some sense satisfied as to "a description of what happens to a large number of grains suspended in an irregularly moving fluid."

We shall try to find $\rho(xyz;t)$ by setting up a "diffusion process." It is the convention to consider diffusion processes as purely continuous. It is certain that some change will occur in any time interval, however small; only, it is certain that the changes during small intervals will also be small.

Define $f(xyz,t_o+\tau;x'y'z',t_o)$ as the probability that a particle definitely located at $x'y'z'$ at time t_o will find itself at x,y,z at time $t_o+\tau$. We can write

$$\rho(xyz,t_o+\tau) = \int_{-\infty}^{+\infty}\int\int\int \rho(x'y'z',t_o)\,f(xyz,t_o+\tau;x'y'z',t_o)\,dx'dy'dz' \qquad (4)$$

It is assumed that the number density $\rho(xyz,t_o)$ is known at some initial instant t_o. The function $f(xyz,t+\tau;x'y'z',t)$ can be considered then as the object of our search.

The function $f(xyz,t_o+\tau,x'y'z',t_o)$, which is often called a transition probability, has the following experimental interpretation. Place a grain at $x'y'z'$ at time t_o and watch where it goes at time $t_o+\tau$. Repeat this experiment an infinite number of times. Each time the grain finds its way into the increment of volume $(xyz,x+dx,y+dy,z+dz)$ record 1, and when it goes elsewhere, record 0. Add the results of each of these experiments and divide

by the number of trials. The limit of this function as the number of trials approaches infinity is assumed to exist and to equal $f\,dxdydz$,

A less abstract interpretation is possible. The experiment is conducted as above except that the position $(x,y,z,)$ at $t+\tau$ is recorded. The following statistics are then calculated:

$$\lim_{N\to\infty} \frac{x_1+x_2+\cdots\cdots x_N}{N} = m_x(x'y'z',t_0+\tau)$$

$$= \iiint x f(xyz,t+\tau;x'y'z',t)\,dx\,dy\,dz$$

$$\lim_{N\to\infty} \frac{(x_1-m_x)^2+\cdots(x_n-m_x)^2}{N} = \sigma_x^2(x'y'z') \qquad (5)$$

$$= \iiint (x-m_x)^2 f(xyz,t+\tau;x'y',z',t)\,dx\,dy\,dz$$

. . . . . .

et cetera. Practically, it is not possible to calculate the limits on the left as $N\to\infty$. However, we can find how large N must be (from small sampling theory) in order that statistics calculated from a finite sample of X's do not have an error greater than that inherent in the measurement of the X's .

Another technique is at our disposal. We can assume that the physical nature of the diffusion process is embodied by some specific mathematical characteristics of $f(xyz,t+\tau;x'y'z',t)$. Chapman and Smoluckowski, for example, assumed that what happened to the grains in one time interval is independent of what happens to them in all other nonoverlapping time intervals. This has proved to be a fruitful assumption if the magnitude of the time interval is properly chosen. In this case the transition probability $f(xyz,t+\tau;x'y'z',t)$ satisfies the integral equation,

$$f(xyz,t+\tau;x'y'z',t) = \qquad (6)$$

$$\iiint f(xyz,t+\tau,x''y''z'',t+s)\,f(x''y''z'',t+s;x'y'z',t)\,dx''dy''dz''$$

Likewise f also satisfies the following conditions,

$$(1)\quad f \geq 0$$

$$(2)\quad \int_{-\infty}^{+\infty}\iiint f\,dx\,dy\,dz = 1 \qquad (7)$$

$$(3)\quad f(xyz,t+\tau,x'y'z',t) \to \delta(xyz;x'y'z')$$
$$\tau\to 0$$

as $\tau\to 0$ where δ is the Diroc delta function.

Now the diffusion processes described by the four conditions above are still rather general. A general solution of the integral equation has yet to be found. However, a general mathematical argument exists which states that the integral equation implies a pair of diffusion equations:

$$\frac{\partial f(xyz,s;x'y'z',t)}{\partial s} = -A_s(xyz)\cdot f(xyz,s;x'y'z',t) \qquad (8)$$

$$\frac{\partial f(xyz;s;x'y'z',t)}{\partial t} = A_t^*(x'y'z')f(xyz,s;x'y'z',t)$$

One equation is a description of the backward process and the other is the forward equation. The symbol $A_u(xyz)$ is a linear operator which acts on the point (xyz) for each time u . $A_u^*(xyz)$ is its "adjoint" operator. If $f(xyz;s,x'y'z',t) = f(s-t,xyz;x'y'z')$ it is said to be stationary. In this case the operator $A_u(xyz)$ operates only upon (xyz) so that

$$A_s(xyz) = A_t^*(xyz) = A_{t-s}(xyz) = A(xyz) \qquad (9)$$

and the pair of diffusion equations becomes:

$$\frac{\partial f}{\partial \tau} = A(xyz)\cdot f(\tau,xyz,x'y'z')$$

$$\frac{\partial f}{\partial \tau} = -A(x'y'z')\cdot f(\tau,xyz,x'y'z') \qquad (10)$$

Multiplying the equations above by $\rho(x'y'z',t)$ and integrating with respect to $(x'y'z')$ gives the single equation for $\rho(xyz,t)$.

$$\frac{\partial \rho(xyz,t)}{\partial t} = A(xyz)\cdot\rho(xyz,t) \qquad (11)$$

The classical heat equation,

$$\frac{\partial \rho(x,y,z,t)}{\partial t} = \sigma^2\left(\frac{\partial^2 \rho}{\partial x^2} + \frac{\partial^2 \rho}{\partial y^2} + \frac{\partial^2 \rho}{\partial z^2}\right) \qquad (12)$$

is an example of a stationary diffusion process. The f corresponding to the $\rho(x,y,z,t)$ in (11), is of the form (10). The telegrapher's equation,

$$\frac{\partial \rho(x,y,z,t)}{\partial t} = \alpha \frac{\partial^2 \rho}{\partial t^2} + \sigma^2\left\{\frac{\partial^2 \rho}{\partial x^2} + \frac{\partial^2 \rho}{\partial y^2} + \frac{\partial^2 \rho}{\partial z^2}\right\}$$

is an example of a nonstationary diffusion process. This equation is known to represent a type of diffusion process since it has been derived from a special random walk problem. It is unfortunate that the theory of nonstationary stochastic processes has not been developed so that special cases of these processes stand alone and in no way help to unify the theory of diffusion.

Let us return to the equation

$$\rho(x,y,z,t+\tau) = \iiint_{x'y'z'} \rho(x,y,z;t)\, f\, dx'dy'dz'$$

Expanding the left-hand side, for small τ

$$\rho(x,y,z;t+\tau) = \rho(x,y,z,t) + \left(\frac{\partial \rho}{\partial \tau}\right)\tau + \left(\frac{\partial^2 \rho}{\partial \tau^2}\right)\frac{\tau^2}{2!} + \left(\frac{\partial^3 \rho}{\partial \tau^3}\right)\frac{\tau^3}{3!} + \cdots \qquad (12)$$

Expanding the right-hand side for small $x-x'$, $y-y'$, $z-z'$,

$$\iiint \rho(x',y',z',t) f\, dx'dy'dz' = \rho(x,y,z,t)\iiint f\, dx'dy'dz'$$

$$+ \frac{\partial}{\partial x}\left\{\rho(x,y,z,t)\iiint (x'-x) f\, dx'dy'dz'\right\} + \frac{\partial}{\partial y}\{\cdots\} + \cdots$$

$$+ \frac{1}{2}\frac{\partial^2}{\partial x^2}\left\{\rho \iiint (x'-x)^2 f\, dx'dy'dz'\right\} + \frac{1}{2}\frac{\partial^2}{\partial x \partial y}\{\cdots\} +$$

$$+ \frac{1}{3\cdot 2}\frac{\partial^3}{\partial x^3}\left\{\rho \iiint (x'-x)^3 f\, dx'dy'dz'\right\} + \frac{1}{3\cdot 2}\frac{\partial^3}{\partial x^2 \partial y}\{\cdots\} +$$

$$+ \cdots\cdots + \text{Remainder} \qquad (13)$$

If it is assumed that

$$a_x(x,y,z,t) = \lim_{\tau \to 0} \frac{1}{\tau}\iiint (x'-x) f(x,y,z,t+\tau; x',y',z',t)\, dx'dy'dz' \qquad (14a)$$

$$\cdots\cdots \text{etc.}$$

$$\sigma_x^2(x,y,z,t) = \lim_{\tau \to 0} \frac{1}{\tau}\iiint (x'-x) f(x,y,z,t+\tau, x',y',z',t)\, dx'dy'dz' \qquad (14b)$$

$$\cdots\cdots, \text{etc.} \quad \text{all exist,}$$

then $$\frac{\partial \rho(x,y,z,t)}{\partial t} = \frac{\partial}{\partial x}\{a_x \rho\} + \frac{\partial}{\partial y}\{a_y \rho\} + \cdots$$

$$+ \frac{1}{2}\frac{\partial^2}{\partial x^2}\{\sigma_x^2 \rho\} + \frac{1}{2}\frac{\partial^2}{\partial y^2}\{\sigma_y^2 \rho\} + \frac{1}{2}\frac{\partial^2}{\partial z^2}\{a_z \rho\} +$$

$$\frac{1}{2}\frac{\partial^2}{\partial x \partial y}\{\sigma_{xy} \rho\} + \cdots\cdots$$

$$+ \frac{1}{6}\frac{\partial^3}{\partial x^3}\{S_x \rho\} + \cdots\cdots \qquad (15)$$

We shall now endeavor to give the moments of f the proper experimental interpretation. If this can be accomplished, we are in a position to impose boundary conditions upon our physical system and to solve the partial differential equation.

The coefficient $a_i(x,y,z,t)$ is the ensemble average displacement of particles. Place a particle at $(x\,y\,z)$ and measure its displacement and position after a time increment τ has elapsed. By repeating the experiment an infinite number of times and averaging, one obtains the theoretical value $\int_0^\tau a_i(x,y,z,t+s)\, ds$. Higher moments of f are obtained in a similar manner, i.e.,

$$\overline{\left\{X^\omega(t+\tau) - X^\omega(t)\right\}^2} \equiv \lim_{N\to\infty} \frac{1}{N}\sum_{\omega=1}^{N}\left\{X^\omega(t+\tau) - X^\omega(t)\right\}^2$$

$$= \int_0^\tau \sigma^2(x,y,z,t+s)\, ds \qquad (16)$$

An alternate approach is to measure the simultaneous displacements of all the particles in the field. Let $X_\alpha(t)$ be the position of the specific particle designated by the number (as contrasted with the experiment number ω). Consider: (the definition)

$$\overbrace{\left\{X_\alpha(t+\tau)-X_\alpha(t)\right\}^p} \equiv \frac{1}{M}\sum_{\alpha=1}^{M}\left\{X_\alpha(t+\tau)-X_\alpha(t)\right\}^p \qquad (17)$$

We can compare the above expression with the moments of f in our theoretical analysis by noting that $X_\alpha(t)$ is the value of some $(x'y'z')$ and $X_\alpha(t+\tau)$ is some value $(x\ y\ z)$ in the function $f(x\,y\,z,t+\tau,x'y'z',t)$. We write then,

$$X_\alpha(t+\tau)-X_\alpha(t) = \int_0^\tau \rho(x\,y\,z,t+s)\,a(x\,y\,z,t+s)\,ds \qquad (18a)$$

$$\left\{X_\alpha(t+\tau)-X_\alpha(t)\right\}^2 = \int_0^\tau \rho(x\,y\,z,t+s)\,\sigma^2(x\,y\,z,t+s)\,ds \qquad (18b)$$

hence

$$\overbrace{\left\{X_\alpha(t+\tau)-X_\alpha(t)\right\}^2} \equiv$$

$$\frac{1}{V}\int_0^\tau \iiint_{x\,y\,z} \lim_{dt\to 0}(x'-x)^2\,\rho(x\,y\,z,t+s)\,f(x\,y\,z,t+s+dt,t+s\ldots)\,dx'\ldots ds$$

where $V = \iiint_{x\,y\,z} dx\,dy\,dz$ (19)

The two previous approaches can be combined in the following way. The experiment is repeated an infinite number of times, but each time the displacements in time τ of all of the particles are measured. The particles are distributed randomly in the field for each experiment. Thus,

$$\overbrace{\left\{X_\alpha^\omega(t+\tau)-X_\alpha^\omega(t)\right\}^2} =$$

$$\frac{1}{V}\iiint_{x\,y\,z}\int_0^\tau \sigma^2(x\,y\,z,t+s)\,dx\,dy\,dz\,ds = 2D\tau \qquad (20)$$

This is the average diffusion coefficient of the entire physical system. If the system were statistically homogeneous in space and time, then

$$\frac{\sigma^2}{2} = D = \text{constant}$$

We have

$$\frac{\overbrace{X_\alpha^\omega(t+\tau)}^{\omega\ 2\ \omega} + \overbrace{X_\alpha^\omega(t)}^{\omega\ 2\ \omega} - \overbrace{X_\alpha^\omega(t+\tau)\,X_\alpha^\omega(t)}^{\omega\ \omega}}{2} \qquad (21)$$

$$= D\tau$$

Now it may be that the combination of space and ensemble averages smooths out the irregularities of the motion too much, thus depriving us of information. However, the above technique affords a method of calculating the diffusion coefficient for a certain total region for the homogeneous case although our actual physical experiment is not homogeneous. We can say, then, that the combination of space and ensemble averages deprives us of the same amount of information as does the assumption of spatial homogeneity.

Thus far our analysis has concerned itself principally with a macroscopic description of a large number of particles from a statistical point of view. As is the case in the kinetic theory of gases, it would be desirable to relate the macroscopic phenomenon to some microscopic hypothesis. In order to make this vital step it is necessary to know something of the behavior of the turbulent fluid in which the particles are suspended. Unfortunately, this information is lacking in both theory and experiment.

In fact, the description of the motion of the suspended particles provides a means of determining an approximate motion of the fluid. We shall, nevertheless, write down an approximate equation relating the suspended particle to the turbulent fluid, hoping that even a coarse description of the fluid will be adequate. Let $\vec{u}(x\,y\,z,t)$ be the fluid velocity and $\vec{V}_\alpha(t)$ the velocity of the α^{th} particle. The simplest equation of motion is:

$$\dot{\vec{V}}_\alpha + \beta\vec{V}_\alpha(t) = \beta\vec{u}(x,y,z,t) \qquad (22a)$$

$$\vec{V}_\alpha(t) = \vec{V}_\alpha(0)\,e^{-\beta t} - \beta\int_0^t e^{-\beta(t-s)}\,u(x(s),y(s),z(s))\,ds \qquad (22b)$$

$$X_\alpha(t+\tau) - X_\alpha(t) = \frac{\vec{V}_\alpha(0)}{\beta}\left\{e^{-\beta t} - e^{\beta(t+\tau)}\right\}$$

$$- \beta \int_t^{t+\tau} \int_0^{t'} e^{-\beta(s-s')} u(x(s), y(s), z(s); s')\, ds'\, ds \qquad (22c)$$

where β is the constant used by Stokes.

$$\left\{X_\alpha(t+\tau) - X_\alpha(t)\right\}^2 = \frac{\vec{V}_\alpha^2(0)}{\beta^2} e^{-2\beta t}\left(1 - e^{-\beta\tau}\right)^2 +$$

$$+\beta^2 \int_t^{t+\tau}\int_t^{t+\tau}\int_0^{s_1}\int_0^{s_2} e^{-\beta(s_1+s_2-s'-s'')} u^\omega(X_\alpha(s'); s') u^\omega(X_\alpha(s''); s'')\, ds'\, ds''\, ds_1\, ds_2$$

$$- 2\vec{V}_\alpha(0) e^{-\beta t} \int_t^{t+\tau}\int_0^{s} e^{-\beta(s-s')} u^\omega(X_\alpha(s'); s')\, ds'\, ds \qquad (23)$$

We are now in a position to average over all particles α, or over all experiments ω, as was done in (16) and (17).

The ensemble number ω is indicated as a superscript of u^ω since it is to be understood that the class of fluid motions determines the class of motions of the $X_\alpha(t)$, except for the initial conditions $X_\alpha(0)$ and $V_\alpha(0)$. When taking the ensemble average, the first term on the left-hand side of (23) is unchanged. The second term is a quadruple integral of a correlation function of the fluid velocities. The third term is double integral of a velocity average.

The average over all the particles α, affects all three terms on the left-hand side. $\overbrace{\vec{V}_\alpha^2(0)}^{\alpha}$ is the average initial energy of the particles. The function $\overbrace{u(X_\alpha(s); s)\, u(X_\alpha(t); t)}^{\alpha}$ is a Lagrangian correlation function which is similar to, but by no means equivalent to, the Euler correlation function defined by

$$\int u(x, s)\, u(x+\rho, t)\, dx \quad \text{say.}$$

If $X_\alpha(s) - X_\alpha(t) = \rho_\alpha$

were the same for all α (in which case spatial homogeneity is implied) and averaging over an infinite number of particles in a finite volume (or a finite number uniformly distributed) then these special Lagrangian and Eulerian correlations are probably equivalent. There is, however, no point in carrying this matter much further until it can be decided how intimate a relation these correlation functions have to the turbulent characteristics of the fluid.

In order to solve the diffusion problem as stated in Eq. (15), say, some boundary conditions are needed. These boundary conditions must be mathematically adequate and physically consistent with those for the fluid. This will not be discussed here, as this point was covered in a previous report by I. Michelson.*

In the next section an incomplete treatment of the motion of an incompressible viscous fluid in a finite box is given. The boundary conditions are particularly simple. The same kind of boundary conditions can be used for Eq. (15). In the next report, this approach will be extended to apply to a water tunnel. Extension to an open channel seems rather remote. Since beginning this report, some additional results have been found which, it is believed, will tend to further integrate the entire field.

B. TURBULENCE IN A RECTANGULAR BOX

Let us consider the motion of a viscous incompressible fluid in a finite box. The box can have any shape one might encounter in physics. So as to facilitate the exposition, let us choose the box to be a rectangular parallelopiped whose edges are L_1, L_2, L_3. On the faces of the box it will be assumed that the velocity of the fluid is $q_{\|}(x, y, z, t) = 0$.

$$\text{Define } E(t) = \int_0^{L_1}\int_0^{L_2}\int_0^{L_3} q_{\|}^2\left(\frac{x, y, z, t}{2}\right) dx\, dy\, dz < \infty \qquad (1)$$

$$R(\rho_1, \rho_2, \rho_3; t) = \int_0^{L_1}\int_0^{L_2}\int_0^{L_3} q_{\|}\left(\frac{x, y, z, t}{2}\right) q_{\|}(\rho_1 - x, \rho_2 - y, \rho_3 - z; t)\, dx\, dy\, dz \qquad (2)$$

where $q_{\|}(-x, y, z, t) = -q_{\|}(x, y, z, t)$ etc.

$$\text{Also define } \Gamma(k_1, k_2, k_3, t) = \int_{-\infty}^{+\infty}\int\int q_{\|}(x, y, z, t) e^{i(k_1 x + k_2 y + k_3 z)}\, dx\, dy\, dz \qquad (3)$$

It follows from Plancheral's theorem that,

---

*See bibliography at end of report.

$$E(t) = \sum_{-\infty}^{+\infty}\sum\sum \Gamma(k_1k_2k_3;t)\Gamma^*(k_1k_2k_3;t) \tag{4}$$

$$R(\rho_1\rho_2\rho_3;t) = \iiint_{-\infty}^{+\infty} \Gamma(k_1k_2k_3;t)\Gamma^*(k_1k_2k_3;t)e^{-i(k_1x+k_2y+k_3z)}\,dk_1dk_2dk_3 \tag{5}$$

Define $F(K,t)$ such that

$$E(t) = \sum_{K_0}^{\infty} F(K,t) \xrightarrow[L_{1,2,3}\to\infty]{} \int_0^{\infty} F(K,t)\,dK$$

Then

$$F(K,t) = \iint_{\sigma_\xi} \Gamma\Gamma^*(\xi_1K,\xi_2K,\xi_3K,t)\,d\sigma_\xi \qquad (\xi_1^2+\xi_2^2+\xi_3^2=1) \tag{6}$$

which implies $K^2 = k_1^2+k_2^2+k_3^2$

Define

$$\mathbb{R}(\rho,t) = \iint_{\sigma_\xi} R(\xi_1\rho,\xi_2\rho,\xi_3\rho;t)\,d\sigma_\xi \qquad (\xi_1^2+\xi_2^2+\xi_3^2=1) \tag{7}$$

$$R(\rho_1\rho_2\rho_3;t) = \sum_0^m\sum_0^n\sum_0^p \frac{(-i\rho_1)^m(-i\rho_2)^n(-i\rho_3)^p}{m!\;\;n!\;\;p!} \iiint_{-\infty}^{+\infty} k_1^m k_2^n k_3^p \Gamma\Gamma^*\,dk_1dk_2dk_3$$

Since $\Gamma\Gamma^*(k_1k_2k_3;t) = \Gamma\Gamma^*(-k_1,-k_2,-k_3;t) \geq 0$

the odd moments of $\Gamma\Gamma^*(k_1k_2k_3;t)$ are zero.

It can be shown that

$$\mathbb{R}(\rho,t) = \int_0^{\infty} e^{-iK\rho} F(K,t)\,dK = \sum_0^{\infty} \frac{(-i\rho)^{2n}}{2n!} \int_0^{\infty} K^{2n} F(K,t)\,dK \tag{8}$$

$$\lim_{\rho\to 0} \mathbb{R}(\rho,t) = E(t)$$

Let $C(\rho,t) = \dfrac{\mathbb{R}(\rho,t)}{E(t)}$

Then

$$C(\rho,t) = 1 - \frac{\rho^2\int_0^{\infty} K^2F(K,t)\,dK}{E(t)} + \cdots \tag{9}$$

$$\overline{K^2(t)} = \frac{\int_{K_0}^{\infty} K^2F(K,t)\,dK}{\sum_{K_0}^{\infty} F(K,t)} = \lim_{\rho\to 0}\left\{\frac{1-C(\rho,t)}{\rho^2}\right\} \tag{10}$$

We can interpret the left-hand side to be proportional to the dissipation, and the right-hand side to be the radius of curvature of the correlation function at $\rho = 0$, when the velocity $q(x,y,z,t)$ is assumed to satisfy the Navier-Stokes equations. If we assume this to be true and if we call the limit $\overline{K^2(t)}$, then

$$-\frac{1}{2\nu}\frac{dE(t)}{dt} = \overline{K^2(t)}\,E(t) \tag{11}$$

$$E(t) = E(t_0)\,e^{-2\nu\int_{t_0}^{t}\overline{K^2(t)}\,dt} \tag{12}$$

Actually, $\overline{K^2(t)}$ is a function of $E(t)$. To determine it exactly is essentially the same as solving the Navier-Stokes equations. For the Navier-Stokes equations

$$\int_{t_0}^{t} \overline{K^2(t)}\,dt \geq 3\pi\left(\frac{1}{L_1^2}+\frac{1}{L_2^2}+\frac{1}{L_3^2}\right) \tag{13}$$

$\dfrac{1}{\sqrt{\overline{K^2(t)}}}$ is the root mean square average diameter of the eddies at time t.

If we use the Navier-Stokes equations to calculate the total kinetic energy in the box, we find

$$0 = \frac{dE(t)}{dt} + \nu\int_0^{L_1}\int_0^{L_2}\int_0^{L_3}\left\{\left(\frac{\partial q}{\partial x}\right)^2+\left(\frac{\partial q}{\partial y}\right)^2+\left(\frac{\partial q}{\partial z}\right)^2\right\}dx\,dy\,dz \tag{14}$$

The integral on the right is a Dirichlet integral and we can find the conditions to minimize it. It is well known that the integral is a minimum when $q(x,y,z,t)$ satisfies the classical heat equation, which is a linearization of the Navier-Stokes equation. Furthermore

$$E(t) \leq E(t_o)\, e^{-2\nu K_o^2 (t-t_o)} \qquad (15)$$

where $K_o^2 = 3\pi\left(\frac{1}{L_1^2} + \frac{1}{L_2^2} + \frac{1}{L_3^2}\right)$

For a nonrectangular shape K_o^2 is the smallest eigenvalue for the Sturm Lioville problem corresponding to that region. We see, then, that in the large, the decay of energy is definitely influenced by the geometry of the system, which is to be expected if partial differential equations are used to describe the system. Since

$$E(t) = \sum_{K_o}^{K_N} F(K, t)$$

it follows:

$$F(K,t_o)e^{-2\nu K_N^2 (t-t_o)} \leq F(K,t) \leq F(K,t_o)e^{-2\nu K_o^2 (t-t_o)} \qquad (16)$$

where K_N^2 is the wave number or eigenvalue corresponding to the smallest eddies in the box. We see at once that the range of eddy sizes is determined forever by the initial conditions. That is, if $F(\lambda, t_o) = 0$, for $K = \lambda$ then $F(\lambda, t) = 0$ for all $t > t_o$.

For large $t - t_o$ the exponentials on the right and left converge so that

$$F(K,t) = F(K,t_o)e^{-2\nu K^2 (t-t_o)} \qquad (17)$$

is a close description of the decay.

BIBLIOGRAPHY

for

Appendix

Bochner, S., "Diffusion Equation and Stochastic Processes," National Acad. of Sci., Vol. 35, No. 7, 1949, pp. 368-370.

Chapman, S., "On the Brownian Displacements of Small Grains Suspended in a Nonuniform Fluid," Proc. of the Royal Society, Series A, 1928.

Michelson, I., "Theoretical Considerations on Turbulent Diffusion and Sedimentation," Calif. Institute of Technology, Hydrodynamics Laboratory Report N-71, October, 1950.

Feller, W., "On the Theory of Stochastic Processes, with Particular Reference to Applications," Berkeley Symposium on Mathematical Statistics, p. 403.